IEA Annex 30 - Marin model teknologi

Afsluttende rapport

EUDP 2010 II - 64010-0460

Energistyrelsen

Rapport

Juli 2014

Denne rapport er udarbejdet under DHI's ledelsessystem, som er certificeret af DNV for overensstemmelse med ISO 9001 for kvalitetsledelse

IEA Annex 30 - Marin model teknologi

Afsluttende rapport

EUDP 2010 II - 64010-0460

Udarbejdet for	Energistyrelsen
Repræsenteret ved	Hanne Thomassen, Projektkonsulent

Horns Rev Vindmøllepark

Projektleder	Hans Fabricius Hansen
Kvalitetsansvarlig	Ole Svenstrup Petersen

Projektnummer	11808937
Godkendt	Ole Svenstrup Petersen
Godkendelsesdato	30. juli 2014
Revision	Endelig: 1.0.
Klassifikation	Åben

DHI • Agern Alle 5 • 2970 Hørsholm
Telefon: +45 4516 9200 • Telefax: +45 4516 9292 • dhi@dhigroup.com • www.dhigroup.com

INDHOLDSFORTEGNELSE

FIGURER

TABELLER

BILAG

1 Introduktion

Denne afsluttende rapport for EUDP-projektet 64010-0460 – Marin Model Teknologi dækker - sammen med en konferenceartikel (/4/) samt DTU Vindenergis afsluttende rapporter (/7/ og /8/) – DHI's aktiviteter og resultater inden for projektet. Projektet har været en del af "Offshore Code Comparison Collaboration Continuation" (OC4) som var et internationalt samarbejde mellem en række virksomheder og forskningsinstitutioner om at sammenligne forskellige computermodeller til aeroelastiske responsberegninger af offshore vindmøller. Projektet har været delt i to faser:

Fase 1: Beregning af en vindmølle på et jacket-fundament

Fase 2: Beregning af en vindmølle på en halvt nedsænkbar flydende platform

Projektet har gennem meget veldefinerede modelspecifikationer og lasttilfælde søgt at skabe grundlag for sammenligning af aeroelastiske koder til beregning af strukturel respons af offshore vindmøller.

DHI har primært arbejdet med analyser af den halvt nedsænkbare platform i fase 2. DHI's bidrag har primært bestået i at levere model og interface til en kobling af DHI's model for bevægelse af flydende legemer, WAMSIM, til DTU Vindenergis aeroelastiske model, HAWC2. Interface og model for den koblede model er beskrevet i DTU Vinds afsluttende rapport: "Benchmark comparison of load and dynamics of a floating 5MW semisub wind turbine, using three different hydrodynamic approaches" (/7/).

Derudover har DHI lavet selvstændige analyser af svingningstest og platformrespons i en regulær og to irregulære bølgetidsserier med DHI's model, WAMSIM, alene. I disse lasttilfælde regnes strukturen, dvs. såvel platform som mølle, som stive legemer. Der regnes da heller ikke med vindlast på møllen i disse tilfælde.

I denne rapport præsenteres resultaterne af sammenligningen af tre lasttilfælde: En regulær bølgetidsserie og to irregulære. I konferenceartiklen: "*Offshore Code Comparison Collaboration Continuation within IEA Wind Task 30: Phase II Results Regarding a Floating Semisubmersible Wind System*" (/4/) præsenteres og sammenlignes med de andre deltageres resultater fra svingningstests.

Projektet har vist, at WAMSIM i de fleste situationer giver resultater i overensstemmelse med andre tilsvarende modeller. Dette gælder for svingningstests og for bevægelser i irregulære bølger, mens modellen ikke fungerer tilfredsstillende i regulære bølger. Dette var dog kendt på forhånd og skyldes den matematiske opbygning af WAMSIM. Der er ligeledes lavet en kobling af DTU Vinds vindmøllemodel HAWC2 og WAMSIM, så der kan tages hensyn til påvirkninger fra både hydro- og aerodynamikken. Denne koblede model har generelt givet resultater i overensstemmelse med andre modeller. Der er dog enkelte eksempler, hvor den giver væsentligt forskellige resultater.

I forbindelse med fase 1 har DHI udført en evaluering af bølgekinematik udregnet ved hjælp af Computational Fluid Dynamics (CFD) samt en validering af DHI's eget program til beregning af bølgelaster på en jacket struktur. Dette arbejde er afrapporteret i henholdsvis Bilag A og B.

2 WAMSIM

2.1 Modelbeskrivelse

WAMSIM er en skibsresponsmodel udviklet af DHI til simulering af bølgeinducerede bevægelser af fortøjede og frit flydende strukturer i tidsdomænet, for eksempel skibe og flydende platforme. De bølgeinducerede kræfter beregnes under antagelse af superposition af langkammede bølger. Resultaterne af hver WAMSIM simulering er givet som tidsserier af flytning (surge), vigning (sway), sætning (heave), rulning (roll), duvning (pitch) og giring (yaw) samt diffraktionskræfter på fartøjet og kræfter i evt. fortøjningsliner. WAMSIM er baseret på frekvensdomæneprogrammet WAMIT til beregning af de hydrodynamiske størrelser, se /1/, /2/ og /3/, og de modellerede strukturer er antaget at være fuldstændig stive. Modellen brugt i dette projekt er vist på Figur 2.1.

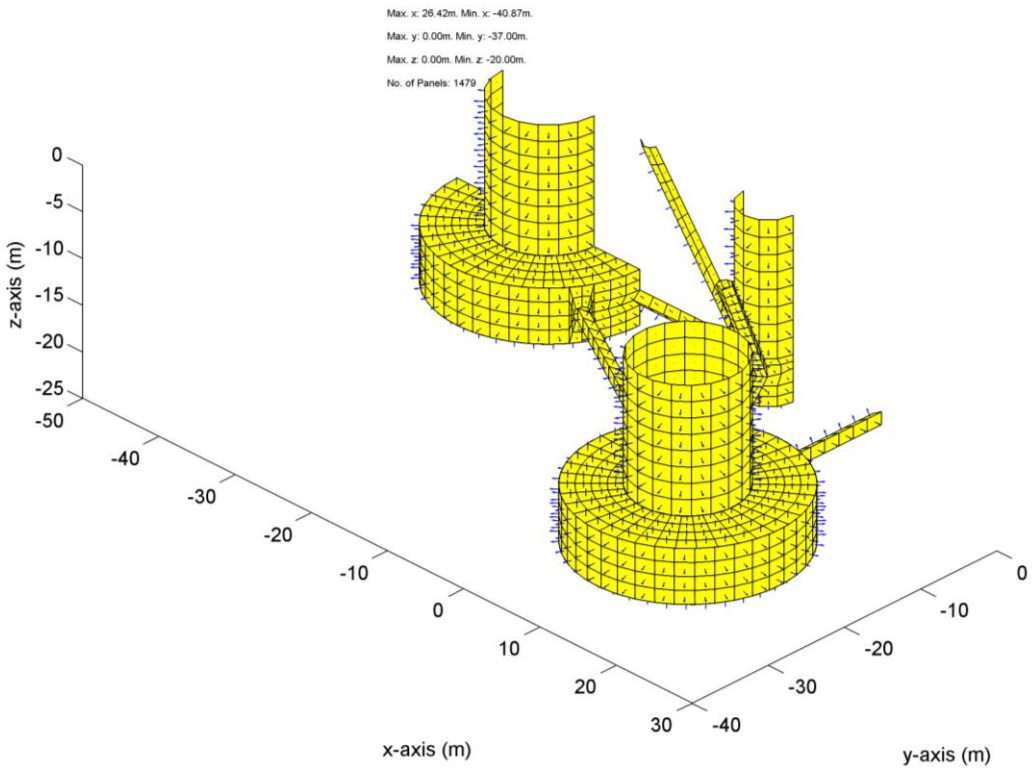

Figur 2.1 WAMSIM modellen af den aktuelle semisubmesible platform. Der er symmetri omkring y=0, hvilket udnyttes til at reducere beregningstiden.

Den følgende korte beskrivelse af WAMSIM er baseret på /3/. Det er antaget, at den hydrodynamiske interaktion mellem væsken og det flydende legeme er fyldestgørende beskrevet med lineær potential teori, det vil sige, at væsken er uden viskositet og rotation i strømningen, samt at den frie overflade og randbetingelserne med det flydende legeme kan beskrives tilfredsstillende til første orden. Med andre ord ignoreres alle ikke-lineære effekter i bølgernes overflade elevation, tryk og kræfter på legemet. Dette kan anses for en god tilnærmelse, så længe $kH/\tanh kh \ll 1$ (hvor k er bølgetallet, H er bølgehøjden, og h er vanddybden). Under antagelse af at legemets bevægelser forbliver små, kan legemets bevægelsesligning opstilles for N frihedsgrader:

$$\sum_{k=1}^{N}\left[\left(M_{jk}+a_{jk}\right)\ddot{x}_k(t)+\int_0^t K_{jk}(t-\tau)\ddot{x}_k(\tau)d\tau+C_{jk}x_k(t)\right]=F_{jD}(t)+F_{jnl}(t),\quad j=1,2...N$$

hvor M_{jk} er massematricen for det flydende legeme, a_{jk} er massematricen for den medsvingende væske, x_k position, hastighed og acceleration af legemet, K_{jk} er en impuls responsfunktion, t er tiden, C_{jk} er den oprettende matrice, F_{jD} er diffraktionskraften på legemet, og F_{jnl} er summen af alle andre kræfter på legemet, inklusiv eksterne ikke-lineære kræfter.

2.2 Sammenligning af resultater med andre OC4 deltagere

Det primære formål med projektet har været at sammenligne resultater fra forskellige numeriske modeller, for derigennem at opnå en bedre forståelse af eventuelle fejl og mangler ved den enkelte model. De første resultater indgår i publikationen: *Offshore code comparison collaboration, continued: phase II results of a floating semisubmersible wind system* (/4/). Artiklen præsenterer resultater fra svingningstests og viser, at WAMSIM modellen giver resultater, der er fuldt sammenlignelige med andre modeller. I dette kapitel bliver tre mere avancerede modelkørsler sammenlignet: En med regulære og to med irregulære bølger. Lasttilfældene indgår i det generelle OC4 program og er defineret i /6/.

2.2.1 Regulære bølger (H=6,0 m og T=10 s)

Lasttilfælde 2.1 omhandler regulære bølger med en bølgehøjde på 6,0 m, bølgeperiode på 10 s og en total varighed på 60 s (dvs. 6 bølgepassager).

WAMSIM er generelt ikke egnet til beregning af skibsbevægelser i regulære bølger. Dette skyldes, at WAMSIM anvender FFT (Fast Fourier Transformation) og inverse FFT på bølge- og responstidsserierne, og dette introducerer betydelige fejl, når det sker på en regulær bølgetidsserie, da en del af energien spredes fra bølgefrekvensen til de omkringliggende frekvenser. Givet dette forbehold, kan tidsserierne af de aktive bevægelsesretninger – flytning (surge), sætning (heave) og duvning (pitch) – ses på Figur 2.2 til Figur 2.4. De resterende retninger – vigning (sway), rulning (roll) og gring (yaw) – bliver ikke aktiveret i langkammede bølger direkte forfra. Dog giver tre til fire andre modeller bevægelser i disse retninger, men der er ikke noget fysisk grundlag for dette.

Det ses af Figur 2.2 til Figur 2.4, at resultatet af WAMSIM beregningerne er i meget dårlig overensstemmelse med de andre modeller, hvilket med stor sandsynlighed skyldes den ovenfor omtalte anvendelse af FFT i WAMSIM. Der er ikke gjort forsøg på at optimere WAMSIM til at håndtere regulære bølger bedre, og konklusionen af resultatet af dette lasttilfælde er, at WAMSIM skal anvendes med meget stor forsigtighed, når det drejer sig om regulære og meget smal-spektrede bølgetidsserier.

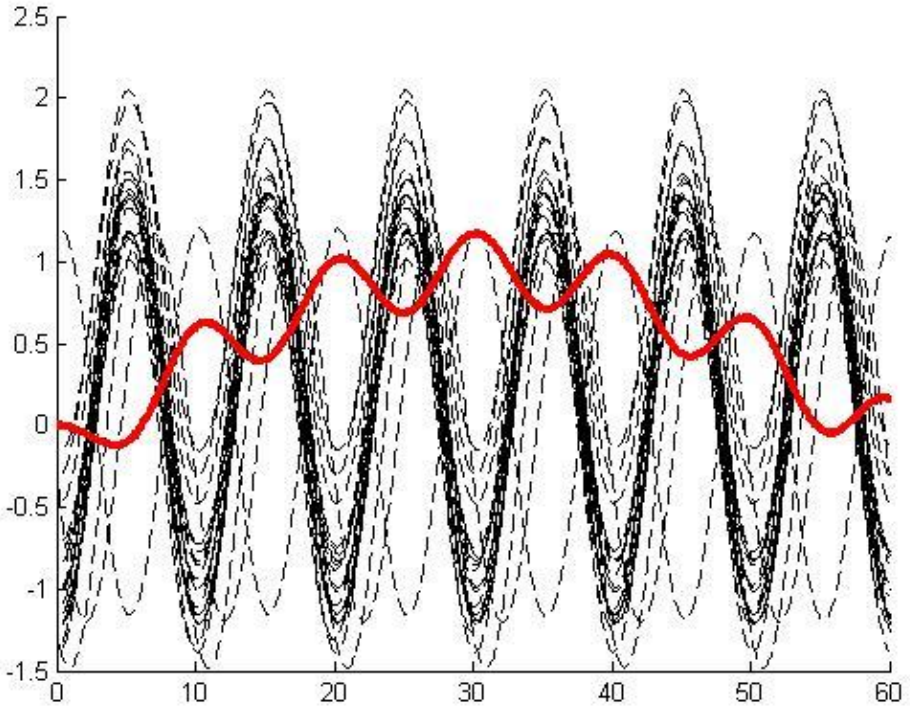

Figur 2.2 Tidsserie for flytningen af platformen. WAMSIM resultatet er markeret med en fuldt optrukket rød linje, mens andre modeller er stipplede sorte linjer.

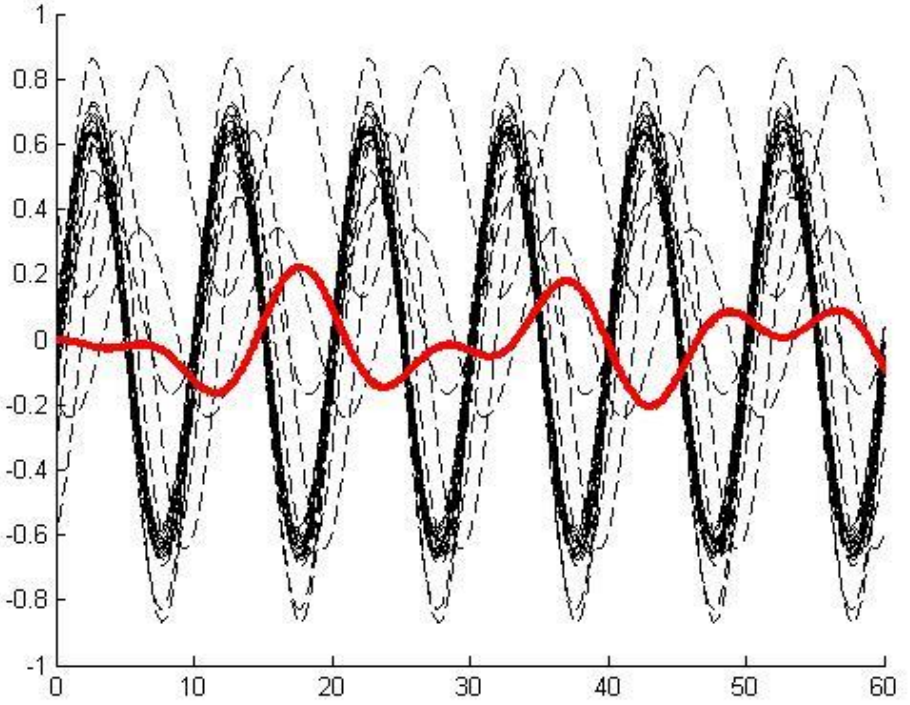

Figur 2.3 Tidsserie for sætningen af platformen. WAMSIM resultatet er markeret med en fuldt optrukket rød linje, mens andre modeller er stipplede sorte linjer.

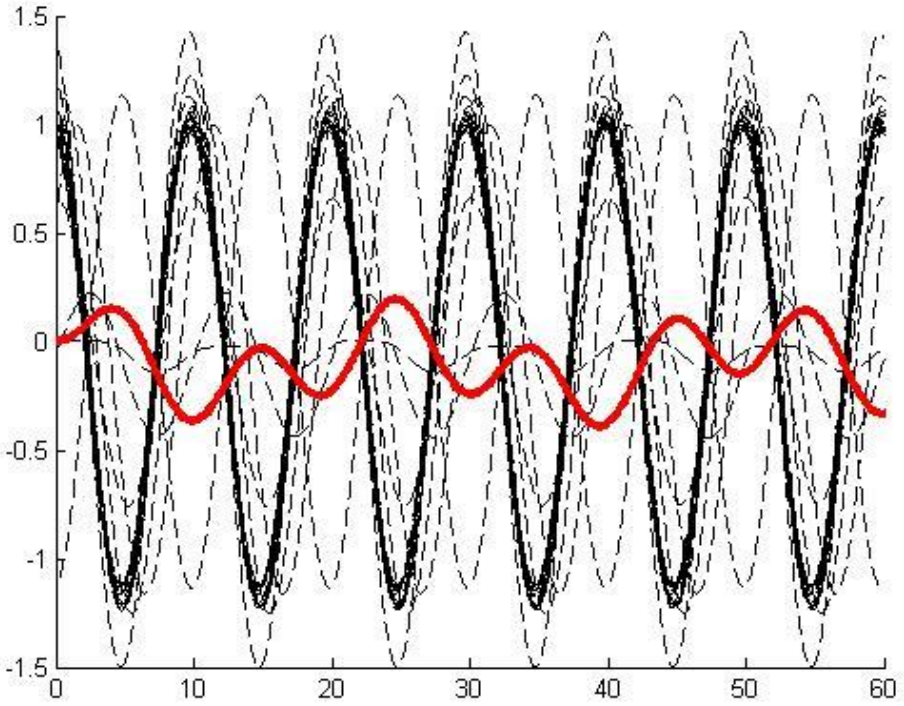

Figur 2.4 Tidsserie for duvningen af platformen. WAMSIM resultatet er markeret med en fuldt optrukket rød linje, mens andre modeller er stipplede sorte linjer.

2.2.2 Lasttilfælde 2.2: Irregulære bølger, H_s=6,0 m og T_p=10 s

Lasttilfælde 2.2 omhandler irregulære bølger med en signifikant bølgehøjde på 6,0 m og en peakperiode på 10 s. Bølgetidsserien er genereret på baggrund af et JONSWAP spektrum med γ=2,87 og er på 60 min. Bølgespektret for tidsserien kan ses på Figur 2.5.

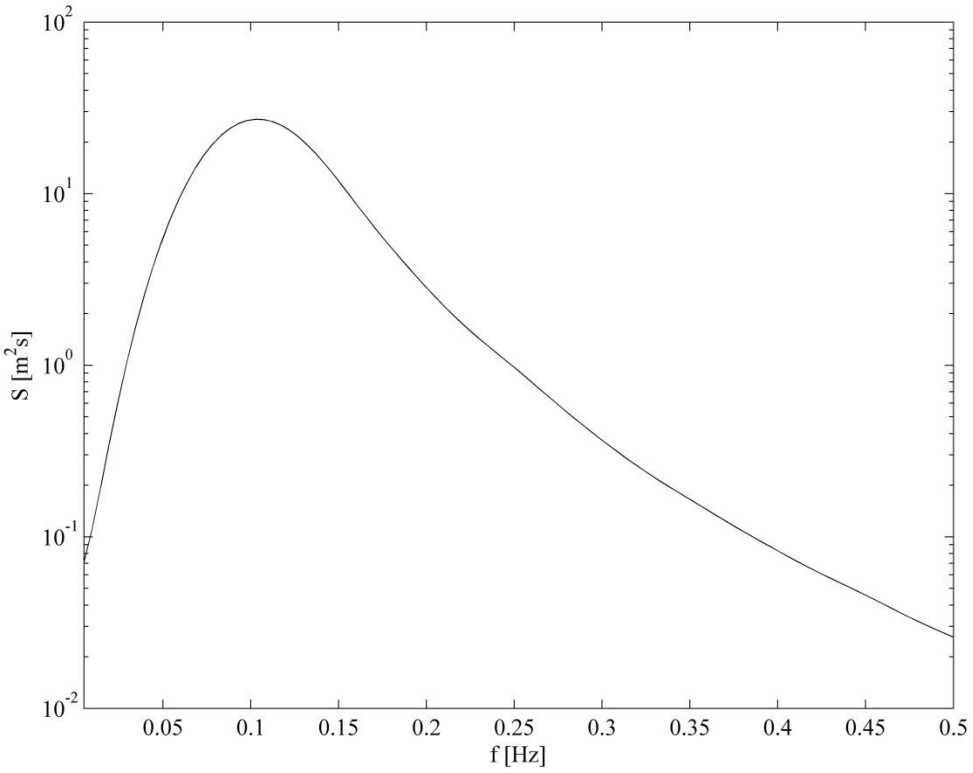

Figur 2.5 Bølgespektrum for lasttilfælde 2.2.

2.2.2.1 Flytning (surge)

Tabel 2.1 viser de karakteristiske værdier for flytning (surge) for lasttilfælde 2.2. WAMSIM ligger blandt en stor del af de andre deltagere med en flytning på ca. ±2,5 m og en standardafvigelse på ca. 0,5 til 0,7 m. Enkelte modeller opnår væsentlig større flytninger. En mulig forklaring på dette kan ses i Figur 2.6. Stort set alle modellerne har to peaks: En omkring 0,01 Hz og en anden omkring 0,1 Hz. Den første peak (0,01 Hz) skyldes egenfrekvensen af hele systemet (platform og fortøjningssystem), se /4/, mens den anden peak er bølgefrekvensen. Hvor stort set alle modellerne giver nogenlunde samme spektralenergi for den direkte bølgeinducerede bevægelse (0,1 Hz), er der meget store variationer, når det kommer til, hvor kraftigt egenfrekvensen af systemet bliver slået an. Dette skyldes sandsynligvis, at nogle modeller inkluderer drift kræfter og andre ikke. Modeller der er baseret på en variant af Morisons formel vil have en positiv middelkraft i bølgeretningen. Det samme vil potential-teori modeller som WAMSIM, hvis anden ordens slow drift kræfter er inkluderet i beregningen. Det er muligt i WAMSIM at inkludere anden ordens slow drift kræfter baseret på den såkaldte Newmans approksimation, men det er ikke gjort i disse beregninger. Derfor er der også meget lidt energi i WAMSIM resultaterne på systemets egenfrekvens, simpelthen fordi denne frekvens ikke anslås i den lineære beregning.

For en designberegning er det vigtigt at tage højde for højere ordens effekter, som kan anslå systemets egenfrekvens, da dette kan være bestemmende for de maksimale ankerkræfter i systemet.

Tabel 2.1 Karakteristiske værdier for flytning (surge) i tilfælde af lasttilfælde 2.2

Kode	OC4 deltager	Maksimum flytning (surge) [m]	Minimum flytning (surge) [m]	Standard afvigelse - Flytning (surge) [m]
WAMSIM	DHI	2.2304	-2.5612	0.6445
OrcaFlex	4Subsea	1.6365	-1.7378	0.5373
CHARM3D+FAST	ABS	5.8360	-3.3060	1.4579
OPASS+FAST	CENER	2.4730	-2.7240	0.7033
FAST	CENTEC	2.0380	-1.8530	0.6042
Bladed	CGC	8.1333	-8.2968	2.6884
FAST	CSIC	1.7740	-1.6540	0.5401
Simo+Riflex+AeroDyn	CeSOS	2.1508	-2.0182	0.5459
HAWC2	DTU	3.0098	-3.9939	0.9943
Bladed Advanced Hydro Beta	GH	2.0500	-1.3700	0.5845
FAST	Goldwind	2.1580	-2.1540	0.6331
3Dfloat	IFE	5.7788	-3.8265	1.1904
FAST	IST	5.5120	-4.3620	1.3635
Riflex-Coupled	MARINTEK	4.4357	-2.3358	0.7820
FAST	NREL	1.6920	-1.7160	0.5819
Hydro-GAST (Morison)	NTUA	3.1588	-2.5292	0.7194
Hydro-GAST	NTUA	2.2050	-2.1395	0.5861
Bladed	POSTECH	10.2958	-7.8357	2.7998
DeepLinesWT (Morison)	PRINCIPIA	3.0248	-1.6261	0.6618
DeepLinesWT (potential)	PRINCIPIA	2.1919	-2.1250	0.6609
SIMPACK+HydroDyn	SWE	1.5890	-1.6489	0.5551
CAsT	Uni. Of Tokyo	2.4749	-3.1858	0.9272
UOU+FAST	Uni. Of Ulsan	2.1500	-2.3700	0.6626
Wavec2Wire	WavEC	1.9116	-1.7938	0.5489

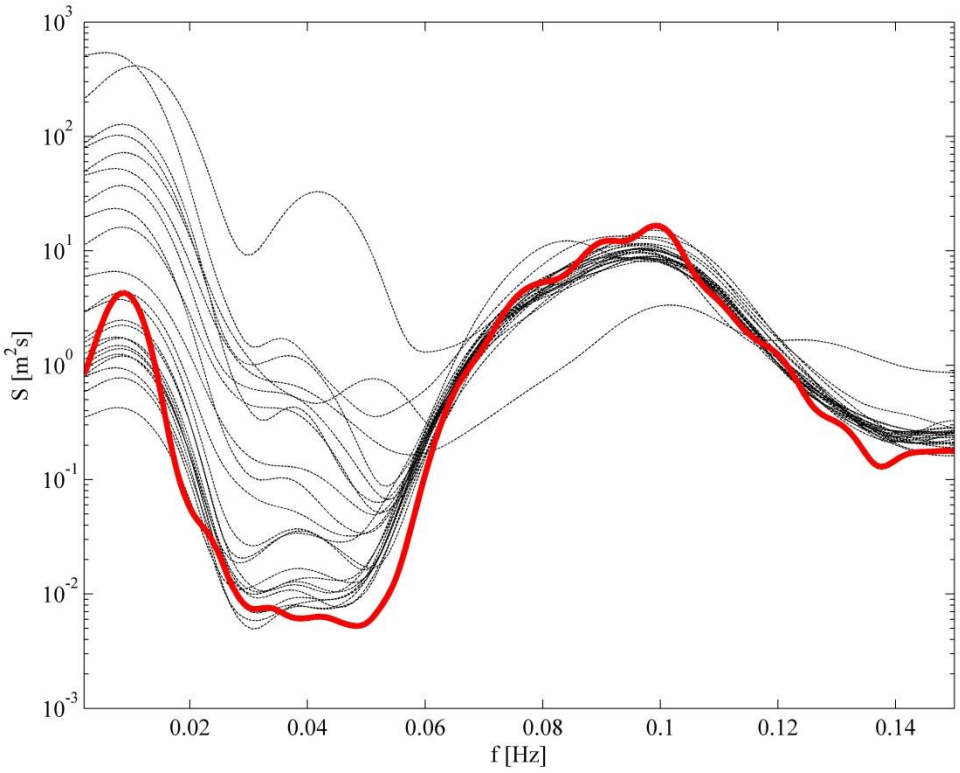

Figur 2.6 Spektrum for flytningen af platformen. WAMSIM resultatet er markeret med en fuldt optrukket rød linje, mens andre modeller er stipplede sorte linjer.

2.2.2.2 Sætning (heave)

Tabel 2.2 viser de karakteristiske værdier for sætning (heave) af platformen. For denne bevægelse har de fleste modeller peak omkring 0,1 Hz (bølgefrekvensen), ligesom de fleste modeller får omtrent samme energi. Der er dog også nogle modeller, der får en betydelig større eller mindre spektralenergi, ligesom peakfrekvensen er lavere i enkelte tilfælde.

Ifølge /4/ er egenfrekvensen af systemet for sætning lidt under 0,05 Hz. Som det ses af Figur 2.7, har langt de fleste modeller generelt ikke meget energi omkring denne frekvens. WAMSIM ligger dog i den lave ende med stort set nul. Det kan skyldes, at ikke alle modeller inkluderer radiationsdæmpningen, dvs. den dæmpning, der opstår som følge af, at den bevægende struktur genererer bølger, som propagerer væk fra strukturen. Det gælder dog for alle modeller, undtagen to, at energien omkring egenfrekvensen af systemet er meget lav, hvilket stemmer overens med, at bølgeenergien i dette frekvensbånd er lille, se Figur 2.5.

Tabel 2.2 Karakteristiske værdier for sætning (heave) i tilfælde af lasttilfælde 2.2.

Kode	OC4 deltager	Maksimum sætning (heave) [m]	Minimum sætning (heave) [m]	Standard afvigelse - sætning (heave) [m]
WAMSIM	DHI	0.9028	-0.9277	0.2585
OrcaFlex	4Subsea	0.8105	-0.7668	0.2582
CHARM3D+FAST	ABS	1.0230	-0.9193	0.2922
OPASS+FAST	CENER	1.1400	-1.2230	0.3069
FAST	CENTEC	0.9318	-1.0250	0.2949
Bladed	CGC	6.2029	-6.1991	1.9080
FAST	CSIC	0.9205	-0.8716	0.2624
Simo+Riflex+AeroDyn	CeSOS	1.2599	-1.2190	0.2768
HAWC2	DTU	1.0650	-1.1105	0.2622
Bladed Advanced Hydro Beta	GH	0.9000	-0.9780	0.2920
FAST	Goldwind	0.8638	-0.8669	0.2789
3Dfloat	IFE	0.8090	-0.8183	0.2947
FAST	IST	1.1150	-0.9222	0.2961
Riflex-Coupled	MARINTEK	1.3629	-1.1681	0.2844
FAST	NREL	0.7418	-0.7185	0.2565
Hydro-GAST (Morison)	NTUA	1.4450	-1.9414	0.4247
Hydro-GAST	NTUA	1.0153	-1.1370	0.2947
Bladed	POSTECH	2.2699	-1.5734	0.6611
DeepLinesWT (Morison)	PRINCIPIA	0.9565	-0.6663	0.2006
DeepLinesWT (potential)	PRINCIPIA	0.8784	-0.8676	0.2570
SIMPACK+HydroDyn	SWE	0.7167	-0.7832	0.2683
CAsT	Uni. Of Tokyo	1.0536	-0.7413	0.2438
UOU+FAST	Uni. Of Ulsan	0.8540	-0.8200	0.2671
Wavec2Wire	WavEC	0.8760	-0.8665	0.2533

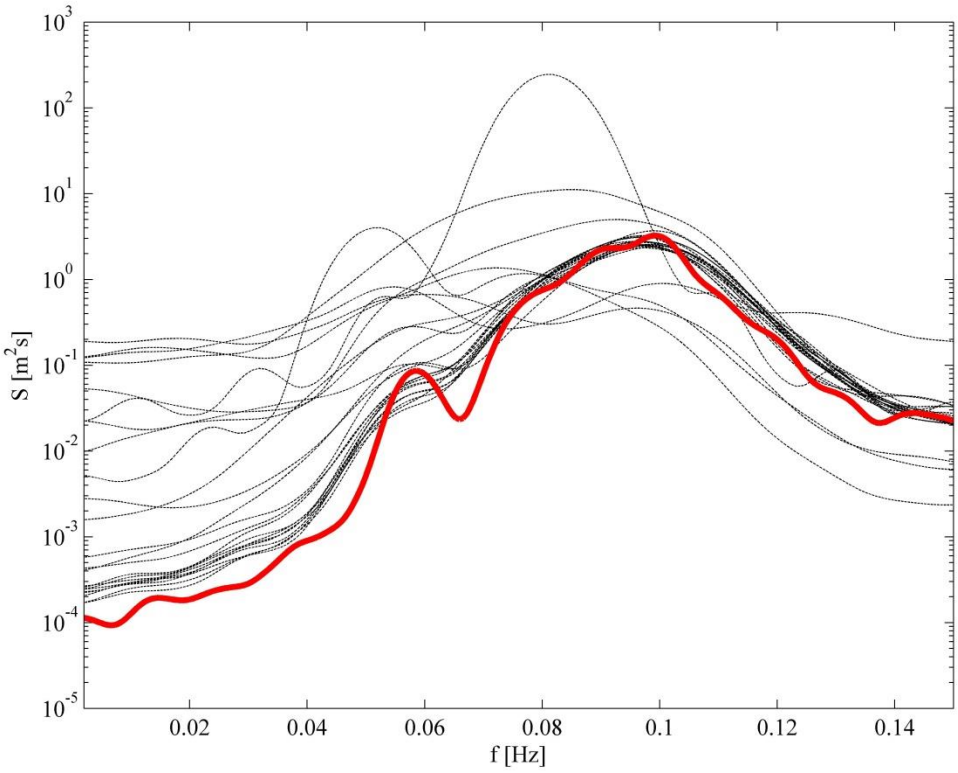

Figur 2.7 Spektrum for sætning af platformen. WAMSIM resultatet er markeret med en fuldt optrukket rød linje, mens andre modeller er stipplede sorte linjer.

2.2.2.3 Duvning (pitch)

De karakteristiske værdier for duvning af platform beregnet ved hjælp af de forskellige modeller er listet i Tabel 2.3. De fleste modeller giver en moderat duvning (standardafvigelse på omkring 0,5° til 1°).

Figur 2.8 viser spektra for duvning af platform beregnet med de forskellige modeller. De fleste modeller beregner en peak omkring bølgefrekvensen (0,1 Hz) og her ligger WAMSIM omtrent midt mellem de andre modeller, måske lidt lavere. En del modeller har desuden en peak omkring 0,04 Hz, som ifølge /4/ er systemets egenfrekvens for duvning. WAMSIM giver stort set ikke nogle bevægelser på denne frekvens, mens andre modeller giver meget store bevægelser. Forklaringen ligger sandsynligvis i fortøjningssystemet samt dæmpningen af hele systemet, ligesom bølgeenergien i dette frekvensbånd er meget lille, ligesom i tilfældet med flytning.

Tabel 2.3 Karakteristiske værdier for duvning (pitch) i tilfælde af lasttilfælde 2.2

Kode	OC4 deltager	Maksimum duvning (pitch) [deg]	Minimum duvning (pitch) [deg]	Standard afvigelse - duvning (pitch) [deg]
WAMSIM	DHI	1.6389	-1.7154	0.4633
OrcaFlex	4Subsea	1.3449	-1.5117	0.4487
CHARM3D+FAST	ABS	1.5340	-1.5510	0.4999
OPASS+FAST	CENER	1.9210	-1.9670	0.5581
FAST	CENTEC	1.6720	-1.5820	0.4847
Bladed	CGC	12.9050	-13.2644	3.7844
FAST	CSIC	1.5960	-1.6510	0.4526
Simo+Riflex+AeroDyn	CeSOS	2.5570	-2.0991	0.5134
HAWC2	DTU	4.4831	-2.7272	0.8655
Bladed Advanced Hydro Beta	GH	0.0255	-0.0274	0.0087
FAST	Goldwind	1.5870	-1.8360	0.5063
3Dfloat	IFE	0.9243	-1.0314	0.2322
FAST	IST	2.6810	-2.4080	0.6923
Riflex-Coupled	MARINTEK	2.5254	-2.2561	0.4950
FAST	NREL	1.3050	-1.4740	0.4665
Hydro-GAST (Morison)	NTUA	1.9189	-2.4532	0.6170
Hydro-GAST	NTUA	1.4132	-1.8445	0.4976
Bladed	POSTECH	2.3868	-3.7506	0.8097
DeepLinesWT (Morison)	PRINCIPIA	2.5274	-2.5862	0.7100
DeepLinesWT (potential)	PRINCIPIA	1.4087	-1.8317	0.4379
SIMPACK+HydroDyn	SWE	1.1899	-1.4185	0.4526
CAsT	Uni. Of Tokyo	1.3939	-1.9075	0.4399
UOU+FAST	Uni. Of Ulsan	2.8300	-3.5300	1.0002
Wavec2Wire	WavEC	1.6056	-1.6784	0.4943

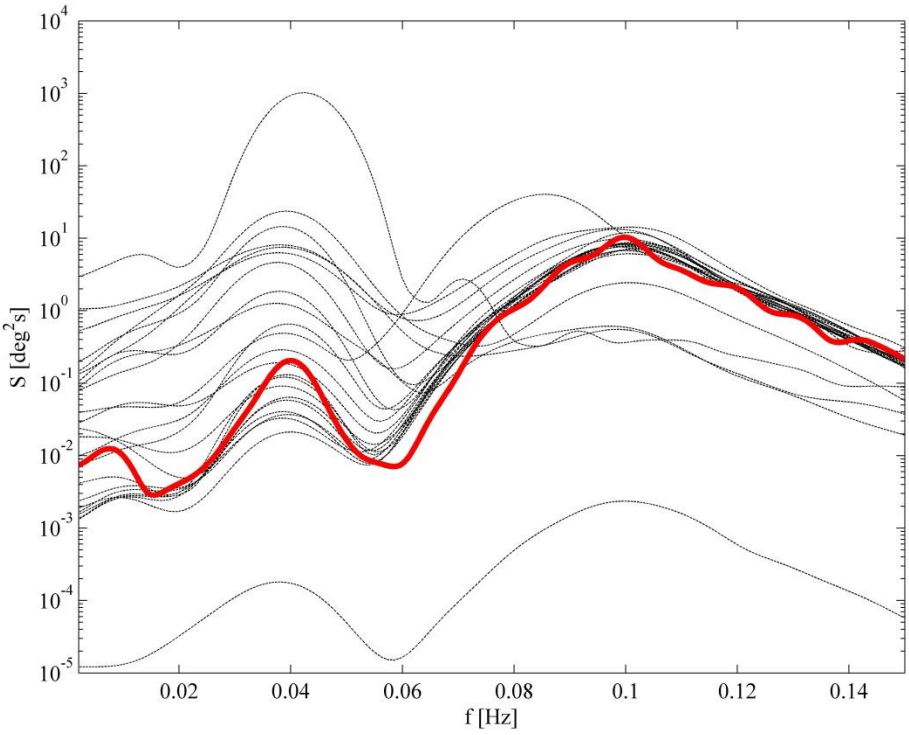

Figur 2.8 Spektrum for duvning af platformen. WAMSIM resultatet er markeret med en fuldt optrukket rød linje, mens andre modeller er stiplede sorte linjer.

2.2.2.4 Vigning, rulning og giring (sway, rolling og yawing)

Opsætningen af modellen gør, at der ikke forventes nogen bevægelse i disse retninger for en potentialteoretisk model som WAMSIM, da kraftpåvirkningen er vinkelret på vigning retningen, bølgerne er langkammede, og den potentialteoretiske model ikke inkluderer viskose kræfter som for eksempel hvirvelafløsning. Resultaterne viser da også, at størstedelen af modellerne – inklusiv WAMSIM – ikke har nogen vigning, rulning eller giring, men enkelte modeller giver mindre bevægelser.

2.2.3 Irregulære bølger (H_s=15,0 m og T_p=19,2 s)

Lasttilfælde 2.5 omhandler irregulære bølger med en signifikant bølgehøjde på 15,0 m og en peakperiode på 19,2 s. Bølgetidsserien er genereret på baggrund af et JONSWAP spektrum med γ=1.05 og længden 60 min. Bølgespektret for tidsserien kan ses på Figur 2.12.

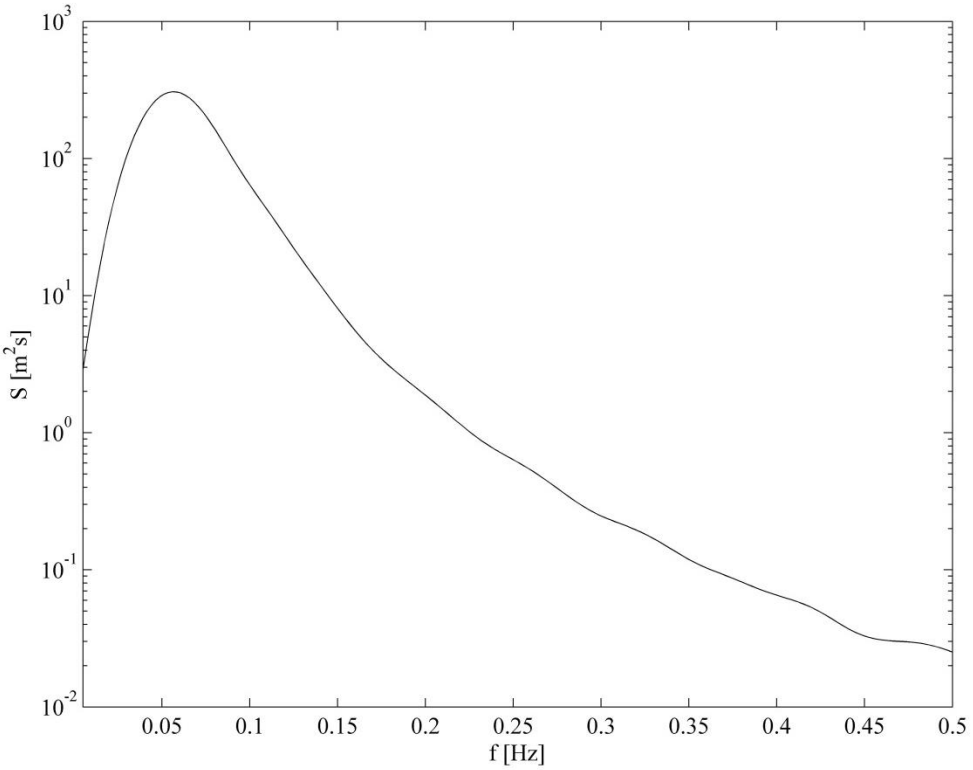

Figur 2.9 Bølgespektrum for lasttilfælde 2.5.

Resultaterne af denne beregning stemmer overordnet med konklusionerne fra kapitel 2.2.2. I dette tilfælde er det ligeledes i flytning, sætning og duvning (surge, heave og pitch) at der sker bevægelser, mens vigning, rulning og giring (sway, rolling og yawing) i stort set samtlige modeller – inklusiv WAMSIM – forbliver upåvirket af samme årsag som beskrevet i kapitel 2.2.2.4.

Der er dog visse variationer i forhold til lasttilfælde 2.2, hvilket ses af flytningsspektra vist på Figur 2.10 til Figur 2.12 (flytning, sætning og duvning). Først og fremmest falder bølgespektrets peakfrekvens til ca. 0,05 Hz. Dette medfører, at bølgefrekvensen og systemets egenfrekvenser kommer væsentlig tættere på hinanden, specielt i tilfælde af sætning. Det ses da også, at specielt sætningen øges markant set i forhold til øgningen i bølgeenergi samt flytning og duvning.

Som i lasttilfælde 2.2 (kapitel 2.2.2) er der en betydelig spredning af resultaterne blandt de forskellige modeller ved beregning af flytning (Figur 2.10), specielt for lave frekvenser. WAMSIM ligger dog stadig i en stor og forholdsvis tæt gruppe af modeller med nogenlunde ens resultater, dog ligger WAMSIM i den høje ende af gruppen omkring platforms egenfrekvens (0,1 Hz).

For sætning (Figur 2.11) ligger WAMSIM ligeledes i midten af en stor gruppe af modeller, ligesom der er et stort sammenfald mellem de beregnede peakfrekvenser omkring 0,05 Hz. Dog har to modeller peakfrekvens mellem 0,07 Hz til 0,08 Hz, hvilket ikke umiddelbart kan forklares, da det hverken passer med platformens egenfrekvens eller bølgeperioden.

For duvning (Figur 2.12) er der en betydelig spredning mellem modellerne. WAMSIM beregner nogenlunde samme energi som det store flertal af modeller, men synes at koncentrere energien på færre frekvenser. Det er dog ikke muligt at sige, hvad der er korrekt på baggrund af tilgængelige data, ligesom det næppe vil have stor betydning i de fleste praktiske anvendelser.

Maksimum, minimum og standardafvigelser for tidsserierne fra de enkelte modeller kan ses i Tabel 2.4 til Tabel 2.6.

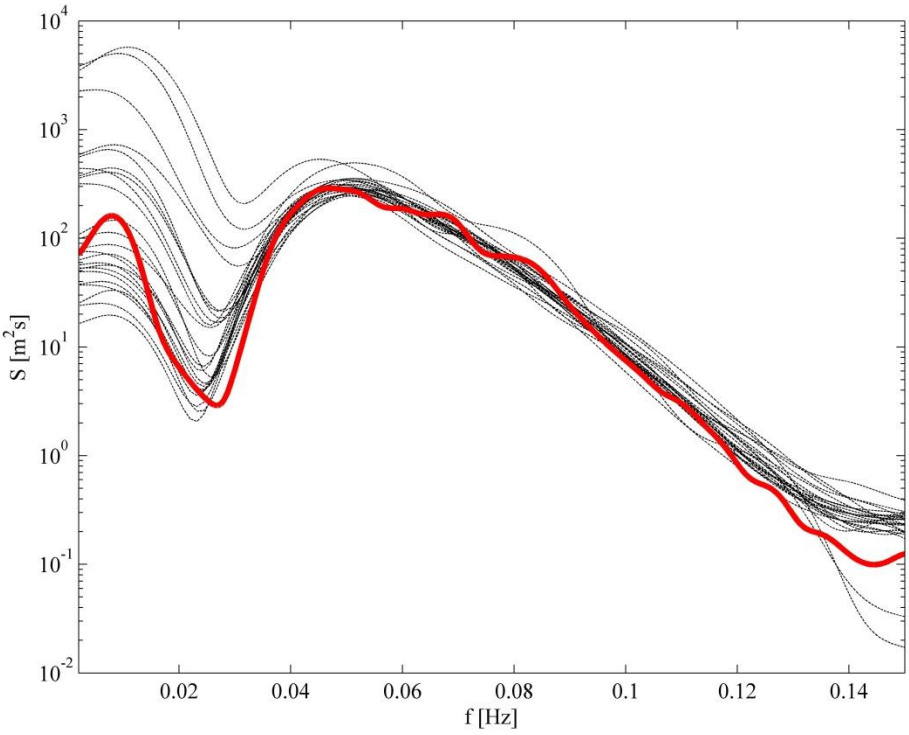

Figur 2.10 Spektrum for flytning af platformen. WAMSIM resultatet er markeret med en fuldt optrukket rød linje, mens andre modeller er stipplede sorte linjer.

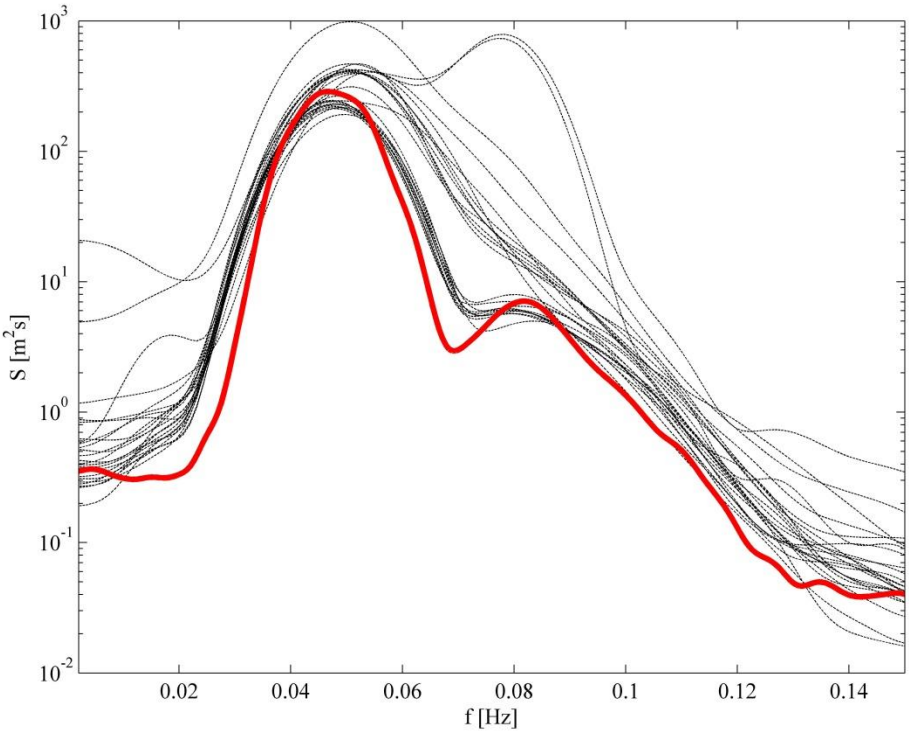

Figur 2.11 Spektrum for sætning af platformen. WAMSIM resultatet er markeret med en fuldt optrukket rød linje, mens andre modeller er stipplede sorte linjer.

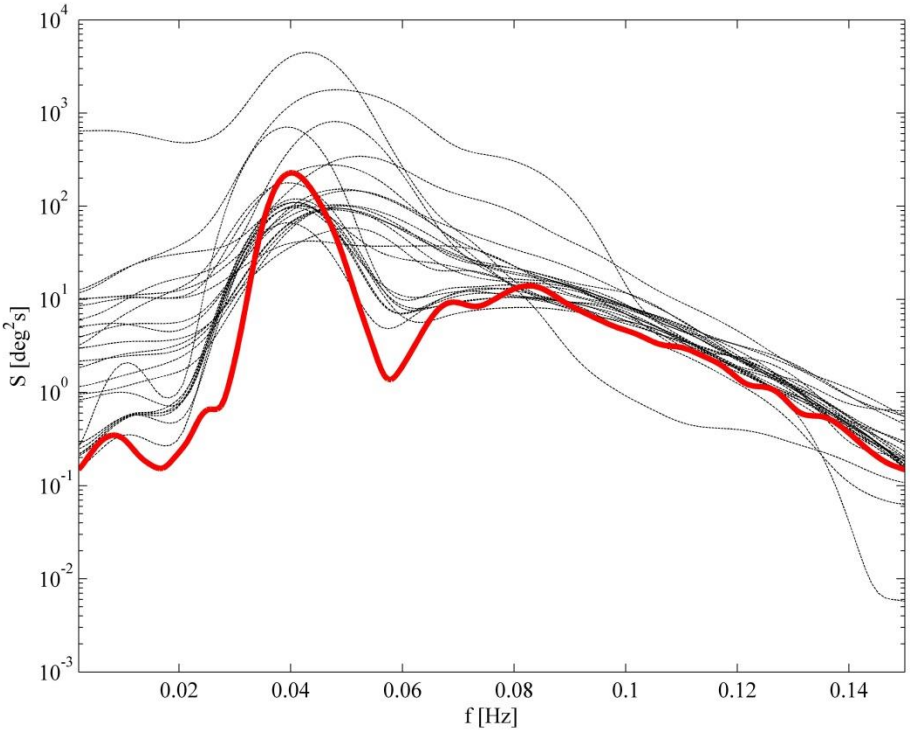

Figur 2.12 Spektrum for duvning af platformen. WAMSIM resultatet er markeret med en fuldt optrukket rød linje, mens andre modeller er stipplede sorte linjer.

De karakteristiske værdier for flytning, sætning og duvning er listet i Tabel 2.4 til Tabel 2.6.

Tabel 2.4 Karakteristiske værdier for flytning (surge) i tilfælde af lasttilfælde 2.5

Kode	OC4 deltager	Maksimum flytning (surge) [deg]	Minimum flytning (surge) [deg]	Standard afvigelse - flyning (surge) [deg]
WAMSIM	DHI	10.0496	-13.1736	3.2030
OrcaFlex	4Subsea	8.9538	-11.5253	3.1203
CHARM3D+FAST	ABS	11.8400	-7.8310	3.2416
OPASS+FAST	CENER	9.8000	-12.6300	3.1927
FAST	CENTEC	10.2100	-10.5800	3.2241
Bladed	CGC	49.5655	-24.2839	10.6115
FAST	CSIC	9.2100	-12.3400	3.0241
Simo+Riflex+AeroDyn	CeSOS	9.0349	-9.9742	2.9942
HAWC2	DTU	19.0479	-9.4839	3.6719
Bladed Advanced Hydro Beta	GH	17.3254	-12.0987	3.7159
FAST	Goldwind	10.6200	-10.0000	3.2093
3Dfloat	IFE	20.6430	-12.0210	4.5781
FAST	IST	9.8750	-9.9630	3.2247
Riflex-Coupled	MARINTEK	10.5410	-7.3900	2.8981
FAST	NREL	9.4650	-9.9760	3.1393
Hydro-GAST (Morison)	NTUA	12.9175	-14.2116	4.1026
Hydro-GAST	NTUA	8.9266	-11.8712	2.9241
Bladed	POSTECH	30.6327	-24.0361	9.6472
DeepLinesWT (Morison)	PRINCIPIA	28.2871	-12.7592	6.7070
DeepLinesWT (potential)	PRINCIPIA	19.9257	-7.3919	4.0759
SIMPACK+HydroDyn	SWE	16.9645	-12.6384	3.6201
CAsT	Uni. Of Tokyo	10.7232	-10.1167	3.0694
UOU+FAST	Uni. Of Ulsan	11.3000	-13.5000	3.9624
Wavec2Wire	WavEC	25.6740	-10.1958	3.9197

Tabel 2.5 Karakteristiske værdier for sætning (heave) i tilfælde af lasttilfælde 2.5

Kode	OC4 deltager	Maksimum sætning (heave) [deg]	Minimum sætning (heave) [deg]	Standard afvigelse - sætning (heave) [deg]
WAMSIM	DHI	6.1710	-6.1940	2.1902
OrcaFlex	4Subsea	5.9040	-6.0689	2.1283
CHARM3D+FAST	ABS	8.9530	-8.8540	3.0226
OPASS+FAST	CENER	9.1710	-9.5620	2.9634
FAST	CENTEC	6.4720	-6.5190	2.1937
Bladed	CGC	15.8404	-16.0695	4.9764
FAST	CSIC	5.1990	-6.0060	2.0311
Simo+Riflex+AeroDyn	CeSOS	9.2505	-9.1281	3.0735
HAWC2	DTU	8.1973	-8.9051	2.6673
Bladed Advanced Hydro Beta	GH	8.7817	-8.6146	2.7058
FAST	Goldwind	6.6160	-6.3770	2.2102
3Dfloat	IFE	10.4980	-9.8729	3.0138
FAST	IST	6.1100	-5.7610	2.2059
Riflex-Coupled	MARINTEK	9.5484	-9.4429	3.0101
FAST	NREL	6.7960	-6.9160	2.2057
Hydro-GAST (Morison)	NTUA	9.8702	-10.6198	3.1249
Hydro-GAST	NTUA	9.7731	-11.6598	3.0265
Bladed	POSTECH	13.1388	-13.4289	4.9479
DeepLinesWT (Morison)	PRINCIPIA	15.3027	-14.4076	4.8261
DeepLinesWT (potential)	PRINCIPIA	10.8183	-12.4694	3.3345
SIMPACK+HydroDyn	SWE	5.6943	-5.2527	2.1148
CAsT	Uni. Of Tokyo	6.9786	-6.9027	2.1764
UOU+FAST	Uni. Of Ulsan	6.0100	-6.0600	2.0890
Wavec2Wire	WavEC	6.1738	-6.9132	2.3370

Tabel 2.6 Karakteristiske værdier for duvning (pitch) i tilfælde af lasttilfælde 2.5.

Kode	OC4 deltager	Maksimum duvning (pitch) [deg]	Minimum duvning (pitch) [deg]	Standard afvigelse - duvning (pitch) [deg]
WAMSIM	DHI	5.4365	-5.9526	1.6144
OrcaFlex	4Subsea	3.4445	-4.1992	1.2428
CHARM3D+FAST	ABS	4.8440	-4.8810	1.4295
OPASS+FAST	CENER	6.1810	-7.1550	1.7740
FAST	CENTEC	8.7810	-9.4030	3.2566
Bladed	CGC	30.1776	-67.9587	9.5937
FAST	CSIC	4.1040	-3.9780	1.4563
Simo+Riflex+AeroDyn	CeSOS	5.4762	-5.4531	1.7725
HAWC2	DTU	8.6131	-10.6322	2.8075
Bladed Advanced Hydro Beta	GH	5.6964	-6.9807	1.5769
FAST	Goldwind	5.3480	-4.7040	1.5175
3Dfloat	IFE	7.0130	-8.7171	1.9247
FAST	IST	6.5390	-5.2920	1.9179
Riflex-Coupled	MARINTEK	6.2031	-5.8690	1.7436
FAST	NREL	4.7750	-4.8330	1.4922
Hydro-GAST (Morison)	NTUA	6.5726	-11.6061	2.3018
Hydro-GAST	NTUA	5.1914	-6.7577	1.7171
Bladed	POSTECH	9.3718	-13.1582	3.3760
DeepLinesWT (Morison)	PRINCIPIA	13.4291	-13.6533	3.9176
DeepLinesWT (potential)	PRINCIPIA	6.9191	-10.1394	2.1250
SIMPACK+HydroDyn	SWE	4.4745	-4.2463	1.4242
CAsT	Uni. Of Tokyo	5.3484	-6.0852	1.5504
UOU+FAST	Uni. Of Ulsan	21.4000	-19.7000	7.2306
Wavec2Wire	WavEC	5.4009	-5.8109	1.6441

3 Kobling af WAMSIM og HAWC2

Som en del af projektet har DHI i samarbejde med DTU Vind arbejdet videre med en kobling af WAMSIM til DTU Vinds aeroelastiske kode, HAWC2. Nogle praktiske problemer med interfacet er blevet løst, og DHI har leveret en WAMSIM model til DTU Vind.

DTU Vind har brugt denne model til at gennemføre beregninger af lasttilfældene i OC4 programmet, defineret i /6/. Resultaterne af beregningerne er rapporteret i /7/ og /8/.

Overordnet set giver den koblede model resultater, der stemmer overens med andre tilsvarende modeller. For nogle frihedsgrader er der dog en betydelig forskel i egenfrekvensen beregnet af den koblede WAMSIM-HAWC2 og andre modeller, når disse findes ved svingningstests, hvilket kan skyldes, at massen i den koblede model ikke er helt korrekt bestemt.

Det ser dog ikke umiddelbart ud til at have nogen indflydelse på resultaterne i tilfælde af irregulære bølgetidsserier, men dette bør givetvis undersøges nærmere, før den koblede model anvendes i praksis.

4 Konklusioner

Fase II af OC4 projektet har vist, at forskellige hydrodynamiske beregningsmetoder leder til betydelige forskelle i resultater, når de anvendes på akkurat samme og meget veldefinerede problem. Det er ikke ud fra de opnåede resultater muligt at afgøre hvilken tilgang, der er at foretrække. Til dette kræves validering mod fysiske modelforsøg eller fuldskalamålinger. Sandsynligvis vil påførte laster skulle beregnes ved en kombination af Morisons formel og potential-teori i praktiske designberegninger.

Beregningerne foretaget med WAMSIM og WAMSIM koblet til HAWC2 viser i hvert fald, at man ikke kan negligere effekten af diffraktion for den her betragtede fundamentstype. De viser desuden, at de hydrodynamiske effekter kan inkluderes i beregningerne uden nævneværdig effekt på beregningstiderne. Det meste af regnekraften skal stadig bruges på den aeroelastiske del af modellen.

5 Henvisninger

/1/ Bingham, H.B.: *A hybrid Boussinesq-panel method for predicting the motion of a moored ship*, Coastal Engineering vol. 40, 2000, pp. 21-38.

/2/ Christensen, E.D., Jensen, B., Mortensen, S.B., Hansen, H.F., Kirkegaard, J.: *Numerical simulation of ship in offshore and harbour areas*. Proceedings of the 27th International Conference on Offshore Mechanics and Arctic Engineering – OMAE 2008.

/3/ Hansen, H.F., Carstensen, S., Christensen, E.D., Kirkegaard, J.: *Multi vessel interaction in shallow water*. Proceedings of the 28th International Conference on Offshore Mechanics and Arctic Engineering – OMAE 2009.

/4/ Robertson, A., Jonkman, J., Vorpahl, F., Popko, W., Quist, J., Frøyd, L., Chen, X., Azcona, J., Uzunoglu, E., Soares, C.G., Luan, C., Yotong, H., Pengcheng, F., Yde, A., Larsen, T., Nichols, J., Buils, R., Lei, L., Nygaard, T.A., Manolas, D., Heege, A., Vatne, S.R., Ormberg, H., Duarte, T., Godreau, C., Hansen, H.F., Nielsen, A.W., Riber, H., Cunff, C.L, Beyer, F., Yamaguchi, A., Jung, K.J., Shin, H., Shi, W., Park, H., Alves, M. and Guérinel, M.: *Offshore code comparison collaboration, continued: phase II results of a floating semisubmersible wind system*. Proceedings of the 33rd International Conference on Ocean, Offshore and Arctic Engineering – OMAE 2014.

/5/ Robertson, A., Jonkman, J., Masciola, M., Song, H., Goupee, A., Coulling, A. and Luan, C. *Definition of the Semisubmersible Floating System for Phase II of OC4,* Dec. 5th 2012.

/6/ Robertson, A., Jonkman, J., Masciola, M., Song, H., Goupee, A., Coulling, A. and Luan, C. *Description of Load Cases for OC4, Phase II*, 27 June 2013

/7/ Larsen, T.J., Yde, A., Verelst, D., Pedersen, M.M, Hansen, A.M., Hansen, H.F.: *Benchmark comparison of load and dynamics of a floating 5MW semisub wind turbine, using three different hydrodynamic approaches*. DTU Wind Energy, 2014.

/8/ Larsen, T.J., Yde, A., Verelst, D., Pedersen, M.M, Hansen, A.M., Hansen, H.F.: *IEA Annex 30 Offshore Code Collaboration Continued (OC4) phase I+II, Final report of the contributions from EUDP 64010-0071*. DTU Wind Energy, 2014.

BILAG

BILAG A – Bølgekinematik

Regulære bølgers kinematik i numerisk bølgerende

WAVE KINEMATICS OF REGULAR WAVE IN NUMERICAL FLUME

1. Introduction

The following work is a part of the 'IEA annex 30 marine model technology' project and furthers a technical note by Bjarne Jensen titled 'Extreme Wave Loads and Run-Up on Circular Cylinder' (APPENDIX1). This report presents a brief investigation to improve the ability of the waveFoam[1] solver implemented in OpenFOAM1.6-ext (OF16-ext) to reproduce wave kinematics when compared to theory.

2. Description of Test Case and Previous Results.

The numerical flume is model is 2D, with a total length of 2000m and a water depth of 50m. "Relaxation" zones are implemented 200m away from the inlet and 200m inside the outlet in order to generate and absorb the wave respectively. For the test cases we have been generating a regular wave using streamfunction theory with the following parameters; wave height H=6m, wave period T=10s and a water depth of h= 50m. A probing location 1200m from the inlet was used to compare calculated velocity against stream function theory. Figure 1 compares the numerical results of waveFoam implemented in both OpenFOAM 2.1 (OF21) and OF16-ext with stream function theory. Previous work had been performed in OF2.1. The reason for testing waveFoam in OF16-ext is so that the features of waveFoam can be integrated with existing OF16-ext solver features for mesh motion and floating bodies. As can be observed from the figure the two implementations are providing reasonably comparable results. Our area of concern is the deviation of the velocity profile from the numerical results to the stream function theory near the free surface (approximately 5m below). This is a known artifact of the surface capturing method implemented with VoF method, which results in the artificially high velocities near the free surface. The numerical mesh for which the results in Figure 1 were calculated is uniform with cells 0.5m*0.5m in dimension.

Figure 2 plots a contour plot of horizontal velocity with the free surface indicated by the white line. It can be seen from the figure the high band of velocity near the free surface, predominately in the air phase. This velocity band is positive throughout the wave period and is the reason for the deviation of the numerical results in both Figure 1 A) and B) from the stream function theory near the free surface.

The following work is all performed in waveFoam implemented in OF16-ext. APPENDIX2 contains OF1.6-ext files for fvSolution and fvSchemes.

[1] waveFoam allows for the generation of waves from various wave theory using openFOAM's VoF solver interFoam as the foundation. Further description is available in Jacobsen t al. (2011).

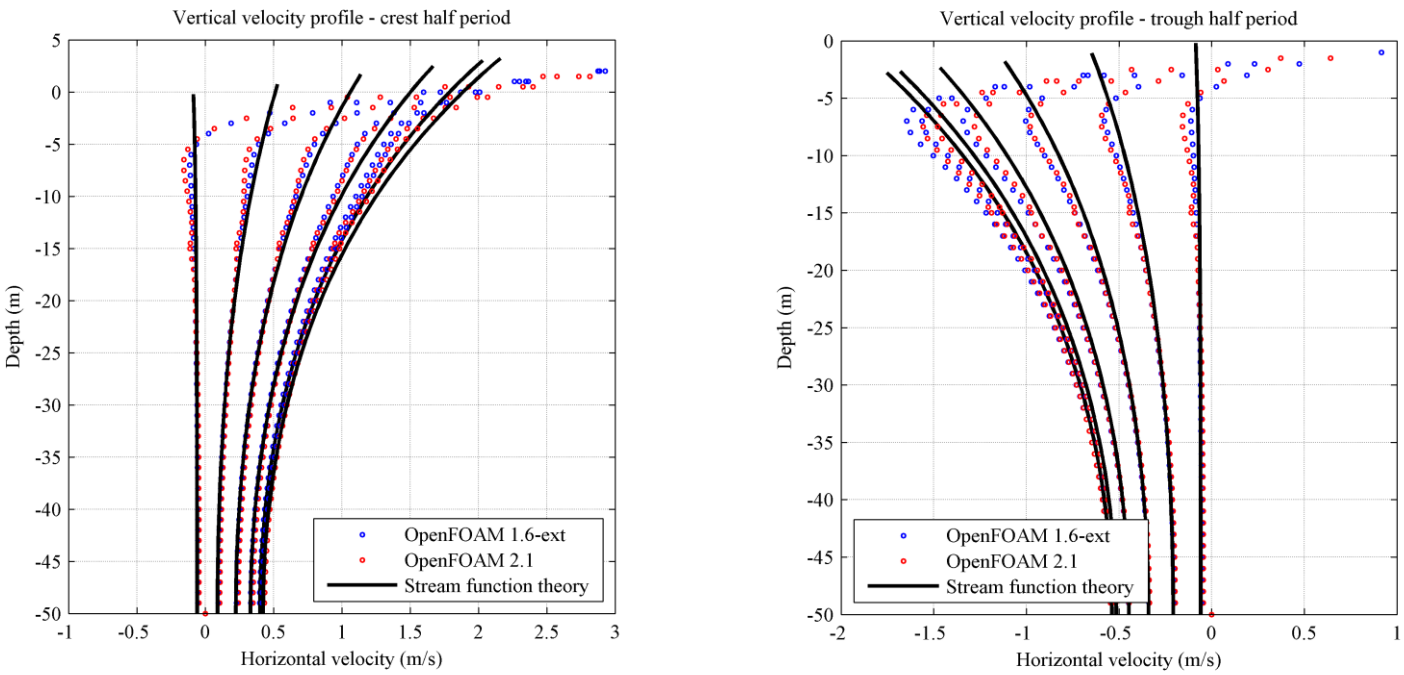

A) B)

Figure 1: Horizontal velocities with respect to height from a vertical probe 1200m downstream of the flume inlet. Plots show comparisons between numerical simulations of waveFoam in OpenFOAM1.6-ext and OpenFOAM 2.1 against streamfunction theory. Plots are spaced with a 0.5s interval. A) Crest half period. B) Trough half period.

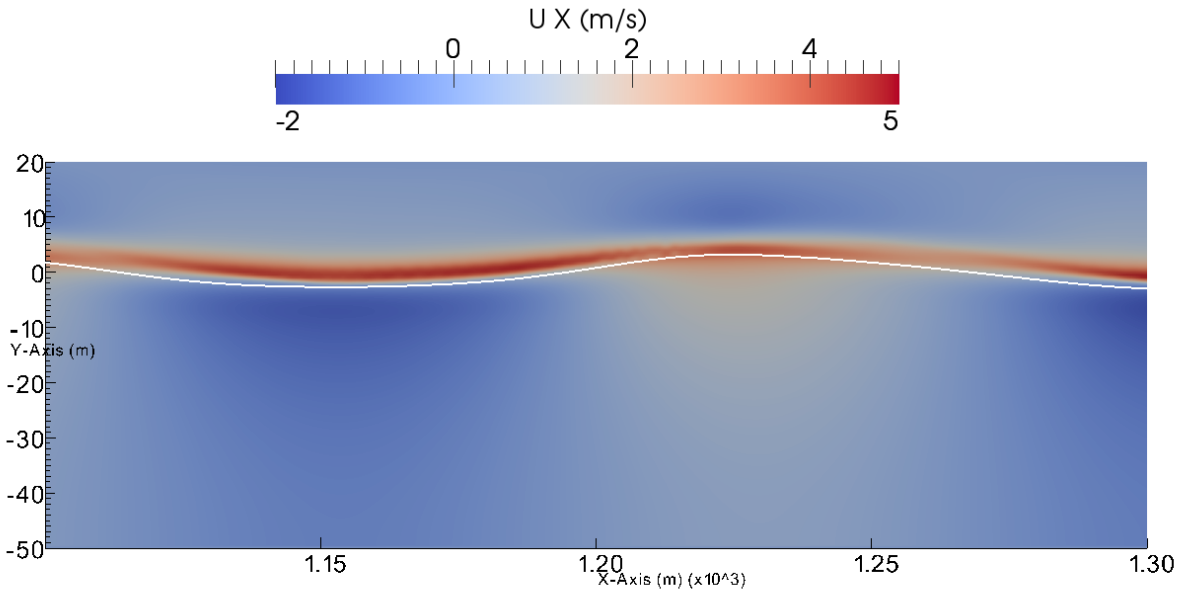

Figure 2: Contour plot of horizontal velocity for a portion of the numerical flume (1100-1300m) at time 200s of the simulation for a propagating streamfunction wave (H=6m, h=50m, T=10s). The white line indicates the free surface.

3. Effect of mesh refinement

In order to limit the effect of the high velocity to the solution, refinement of the mesh around the free surface was proposed. Two meshes were considered which refined the mesh from the uniform base case (results presented in the previous section) with cells of 0.5m*0.5m. The first (Mesh1) of which was refined only the vertical direction resulting in cells measuring 0.1m in the vertical direction while maintain 0.5m length in the horizontal. The second (Mesh2) further refined the vertical cells to a height of 0.05m and lengthwise to 0.17m. Both meshes applied the refinement only to the region of the free surface (±5m from 0m) to avoid the inclusion of unnecessary small cells elsewhere in the domain. The base mesh consisted of 560000 elements with a maximum aspect ratio of 1, Mesh1 contained 1000000 elements with a maximum aspect ratio of 4.5, while Mesh2 contained 4080000 cells with a maximum aspect ratio of 4.33. All meshes are in 2D. Table 1 below summaries the above text.

	Number of Cells	Cells size at free surface	Max aspect ratio	Graded/Uniform
Base Mesh	560000	0.5m (Horizontal) * 0.5m (Vertical)	1	Uniform
Mesh1	1000000	0.5m (Horizontal) * 0.1m (Vertical)	4.5	Graded
Mesh2	4080000	0.17m (Horizontal) * 0.05m (Vertical)	4.33	Graded

Table 1: Description of 2D computational meshes.

Figure 3 plots the improvement of the numerical solution to the theory with refinement around the free surface compared to the base mesh. It is evident from the plot that the further refinement of Mesh2 shows at times a slight if not negligible improvement when compared to the less refined Mesh 1 (the numerical solution of Mesh2 deviates from the theory at a point slightly closer to the free surface). One has to be aware of the impracticality of the questionable gain in accuracy to the significantly increased numerical cost of decreasing the cell size (over 4 times the number of cells to Mesh1). The presence of the high velocity still makes this current model unsuitable for modeling near surface wave kinematics.

Figure 4 plots the contour plot for the solution from the most refined mesh (Mesh 2), for a portion of the flume 1100m-1300m downstream of the inlet. Similar to result plotted from the base mesh (Figure 2), we can still observe the high velocities around the free surface, causing the deviation of numerical results from theory in Figure 3.

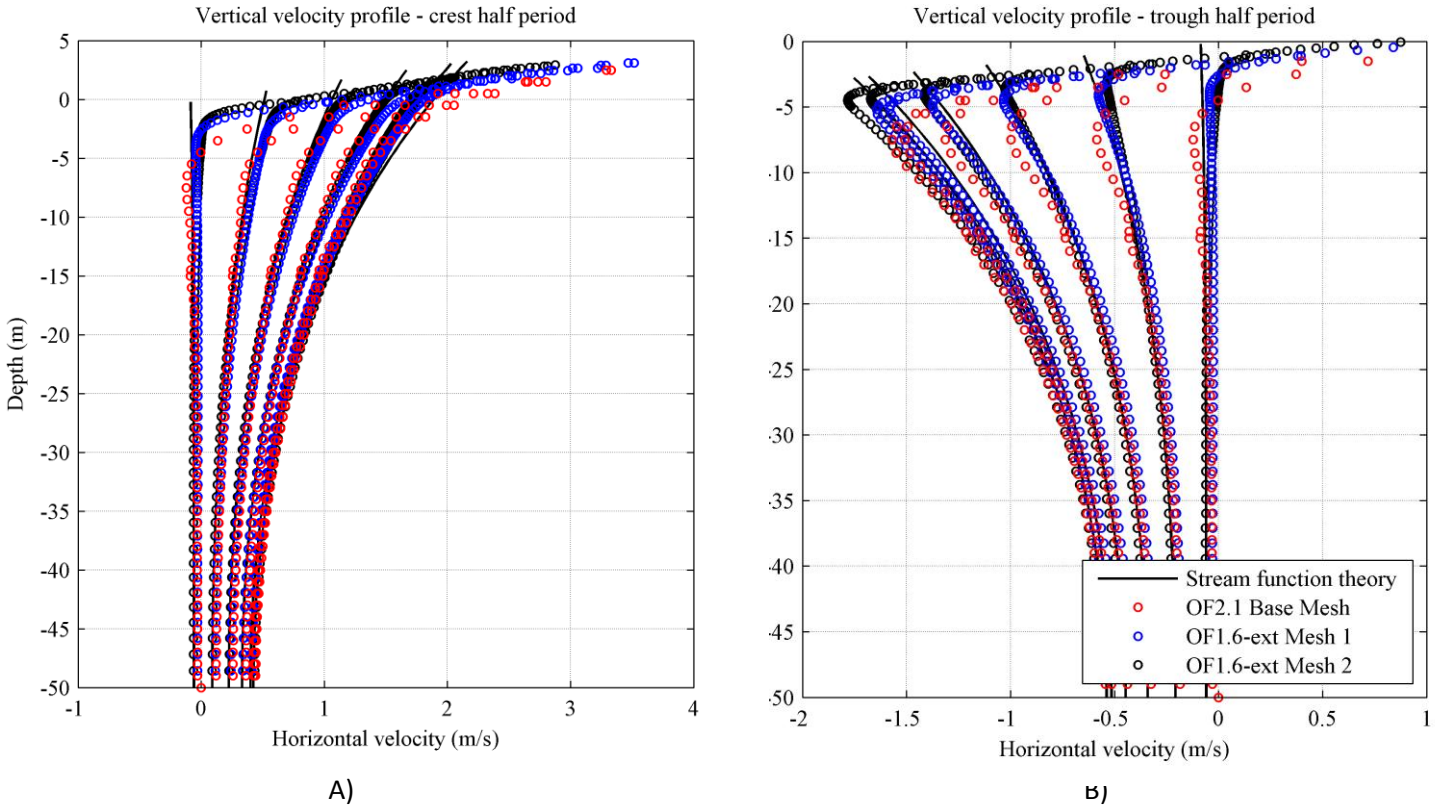

Figure 3: Horizontal velocities with respect to height from a vertical probe 1200m downstream of the flume inlet. Plots show comparisons between two numerical simulations of two meshes (Mesh 1 and Mesh2) in waveFoam in OpenFOAM1.6-ext and the base mesh modelled in OpenFOAM 2.1 against streamfunction theory. The base mesh has uniform cell size of 0.5m*0.5m, Mesh 1 has cells of size 0.5m*0.1m around the free surface and Mesh 2 has cells of 0.17m*0.05m around the free surface. Plots are spaced with a 0.5s interval. A) Crest half period. B) Trough half period.

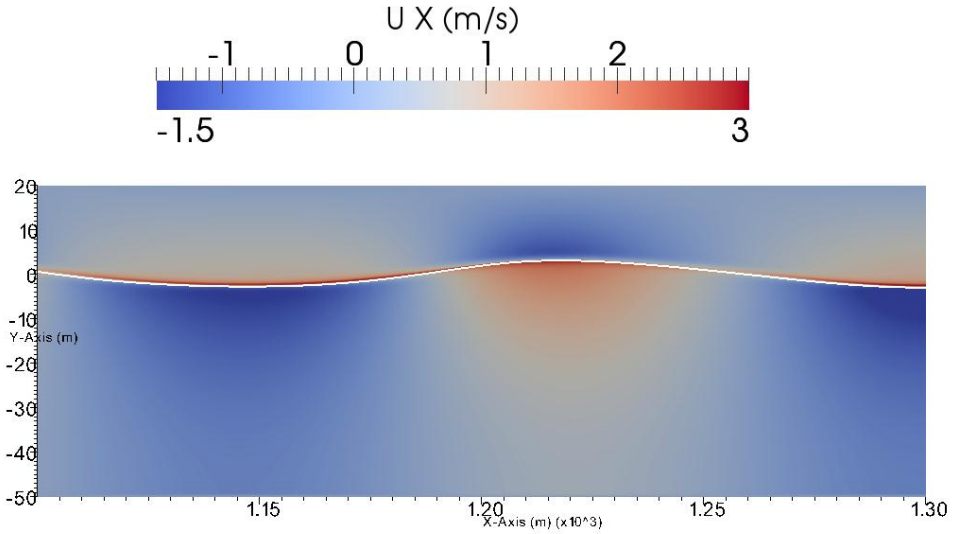

Figure 4: Contour plot of horizontal velocity for a portion of the numerical flume (1100-1300m) at time 200s of the simulation for a propagating streamfunction wave (H=6m, h=50m, T=10s). The white line indicates the free surface. (Mesh2)

4. Comparison with 3D model

In order to test if the high velocities near the surface are evident in a 3D model, Mesh1 (Table1) was extended to have a thickness of 1m with a discretization of 5 elements. Similarly, a probe at 1200m downstream was used to compare velocity results to the 2D version of Mesh1. Figure 5 below shows that no difference can be observed between the model the 2D and 3D versions of Mesh1.

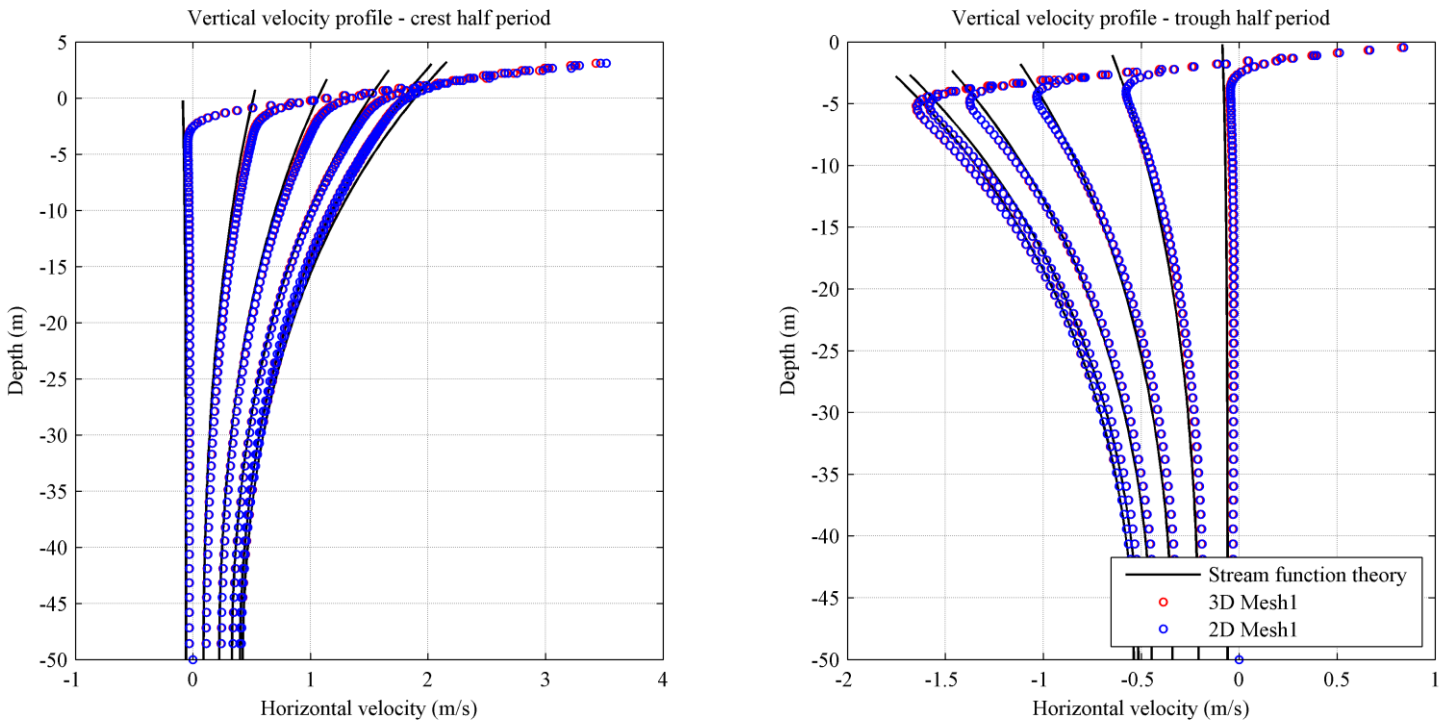

Figure 5: Horizontal velocities with respect to height from a vertical probe 1200m downstream of the flume inlet. Plots show comparisons between two numerical simulations of two meshes (3DMesh 1 and 2D Mesh 1) in waveFoam in OpenFOAM1.6-ext against streamfunction theory. . Plots are spaced with a 0.5s interval. A) Crest half period. B) Trough half period.

5. Conclusions

- We have been able to model the progression of a regular streamfunction wave using waveFoam implemented in OF16-ext. The kinematics of this wave 1200m downstream of the flume inlet compares well except for close to the free surface where artificially high velocities exist (an artifact of the implemented VoF method).
- Mesh refinement limits the influence however does not exclude it. Accurate representation of wave kinematics is essential for modelling offshore structures.
- Future work might consider are other free surface handling schemes which are able to handle the density gradient at the interface. Other options would be to eliminate the air phase and solve the wave motion as a single phase, excluding unphysical gradients in density.

6. References

Jacobsen, N.G Fuhrman, D. R., & Fredsøe, J. (2011). A wave generation toolbox for the open-source CFD library: OpenFOAM. *International Journal for Numerical Methods in Fluids.* Doi:10.1002/fld.

APPENDIX1: Bjarne Jensen's Technical Note

Technical Note on

Extreme Wave Loads and Run-up on Circular Cylinders

1. INTRODUCTION

The present technical note describes the work performed as part of the projects "Wave Loads on Offshore Wind Turbine Foundation" and "IEA annex 30 marine model technology". The work forms a first test and validation of the OpenFOAM code for offshore marine applications.

The main focus has been put on the circular cylinder case. Cylindrical structures are widely used within the marine and offshore area. Examples are pipelines, risers, and platform jacket legs within the oil and gas industry, mono-piles and caisson foundations for offshore wind turbines as well as infrastructural constructions such as bridge piers. When applying a numerical model for evaluation of the flow around, and forces on, these structures it must be shown that the model is capable of reproducing the physics and corresponding physical response of the structure. In this note three topics are investigated: 1) simulation of the undisturbed wave kinematic on a flat bed for regular stream function waves as well as irregular waves, 2) forces on a vertical cylinder in large (extreme) waves and, 3) run-up on a vertical cylinder.

The note is organized with the following sections. In Section 2 a brief background for the model is given as well as for the wave generation toolbox, waves2Foam, which has been adopted as wave boundary condition for the present work. In Section 3 it is shown how the OpenFOAM model can be used for generating irregular wave kinematics for use in for example load calculations on offshore structures. Section 4 shows an example of direct evaluation of forces on circular cylinders from non-linear waves. Here the NS3 code is applied for generating reference results to which the OpenFoam results are compared with good agreement. In Section 5 the run-up on the circular cylinder is investigated by comparison to experimental results.

2. NUMERICAL MODEL AND WAVE GENERATION

The work summarized in the present note includes CFD modeling based on the NS3 code developed at DHI and the open source code OpenFOAM. The main part of the work is based on the OpenFOAM code while the NS3 code is applied for generating reference results. Common for both models is the combination of a numerical solution of the Navier-Stokes equations, a Volume of Fluid (VOF) free surface description and a wave generation and absorption boundary condition.

The NS3 model is based on the finite volume method for general non-orthogonal mesh. The solver was described in Mayer et al. (1998) and was later extended with the VOF method based on the originally developments by Hirt and Nichols (1981). The model

has been validated and applied in numerous projects involving offshore and marine applications where free surface flow and wave modeling is essential. For the present work the NS3 model is applied for generating reference results of wave forces on a vertical cylinder to which the results of the OpenFOAM model is compared.

The OpenFOAM model is, as the NS3 model, based on the finite volume method. For the present work the resent version 2.1.0 is applied which is released and maintained by OpenCFD®. Wave modeling is adopted by the wave generation frame work waves2Foam. The development of this frame work was part of Jacobsen (2011) while it is further described in Jacobsen et al. (2011).

3. WAVE KINIMATICS AND IRREGULAR WAVES

A well-known method for establishing design wave forces on offshore structures such as jacket legs, boat landings, bracings etc. is the application of the Morison-equation in combination with an undisturbed wave kinematic. This approach is described in for example Gronbech et al. (2001) and Sterndorff (2002). The wave kinematics to be applied on the individual elements of the structure may be chosen based on regular waves such as Stokes 5^{th} order theory or stream function theory for the given design wave condition. However, some uncertainties lie in this approach as this is not the conditions which is generally experienced at the offshore locations. In this section it is demonstrated how the OpenFOAM model may be applied to generate the undisturbed wave kinematics of an irregular wave condition. In order to show the ability to reproduce the kinematics of free surface water waves a stream function wave is simulated and compared to the stream function theory.

A stream function wave is simulated with the following characteristics. Wave height, H=6m, wave period, T=10s, water depth, h=50. A 2-dimensional model domain is setup with a total length of 2000m. At the inlet and outlet boundary a relaxation zone with a length of 200m is used for generating and absorbing the waves respectively. Two grid resolutions have been tested; uniform spacing of 1mx1m and 0.5mx0.5m which gives a total of 140,000 and 560,000 computational cells. The wave kinematic is extracted over a vertical line at a distance of 1000m from the inlet relaxation zone i.e. the wave has travelled approximately 6.5 wave lengths.

Figure 1 presents the velocity profiles compared to stream function theory for the model with uniform grid spacing of 0.5mx0.5m. The profiles are presented with a spacing of 0.5s corresponding to a phase angle of 18deg. For the most part of the water column the model is seen to give a good representation of the kinematics. However, near the surface a considerable deviation is seen. This is caused by the current VOF implementation which suffers from a physical incorrect interpolation routine for the computational cells where the free surface intersects. The result hereof is the generation of artificially high velocities in the air phase just above the free surface. If the grid resolution is rather course the free surface will be smeared over several computational cells and the

artificial air velocity will have an effect on the fluid phase in these cells. This effect will decrease for refinement of the grid. Based on the results for stream function waves it is concluded that the model will provide a good representation of the wave kinematics although care should be taken when interpreting near surface velocities.

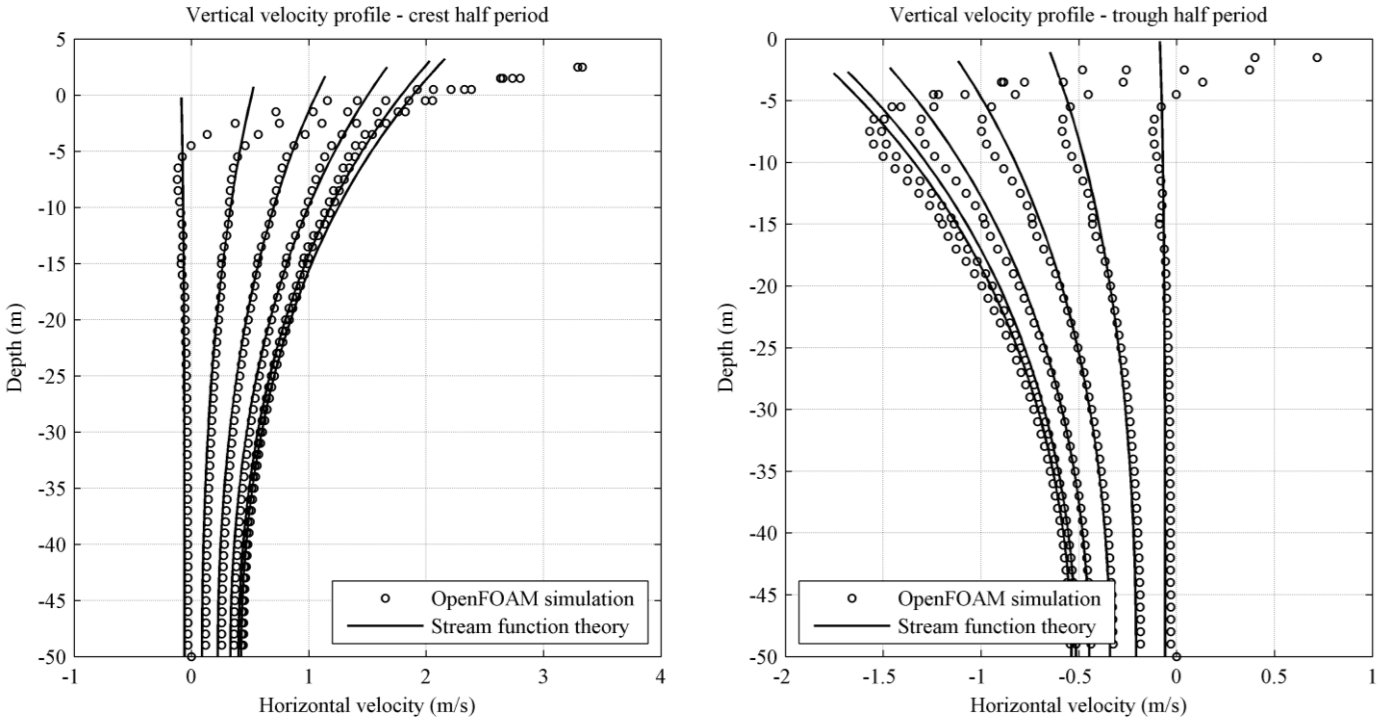

Figure 1. Horizontal velocities for simulated stream function wave compared to theory. Profiles are spaced with 0.5s corresponding to a phase angle of 18 deg. Left panel: crest half period. Right panel: trough half period.

Following the initial validation of the capabilities of the model to reproduce the kinematics of free surface water waves it is demonstrated how the kinematics of an irregular wave condition can be generated and extracted for further use in load calculations on offshore structures. The irregular wave condition is chosen to be based on the Pierson-Moskowitz spectrum. A routine for generation of an irregular wave boundary condition based on a spectrum is available in the applied waves2Foam frame work. A wave condition with the following characteristics has been specified. Significant wave height, H_s=6m, peak wave period, T_p=10s, water depth, h=50m. The computational setup is otherwise identical to the above described setup for simulation of stream function waves. The irregular wave train is propagated into the domain and again the results are extracted at a distance of 1000m from the inlet.

Figure 2 presents the surface elevation time series. Based on the surface elevation a spectral analysis is performed in order to evaluate the wave spectrum compared to the target Pierson-Moskowitz spectrum. Figure 3 presents the target wave spectrum as well as the simulated spectrum at a distance of 200m and 1000m downstream the inlet. It is

seen that the peak wave period is maintained throughout the domain. The significant wave height is decreased with generally to little energy on the higher frequencies to the right of the peak frequency. There may be several explanations to this. The most likely explanation can possible be sought in relation to the spatial resolution of the computational grid. Here a clear weakness was seen as described for the stream function kinematic tests where large artificial velocities were generated in the air phase above the free surface. This effect will cause energy to be diffused out of the system which again will result in decreasing wave heights. Further refinement and optimization near the free surface may reduce this problem.

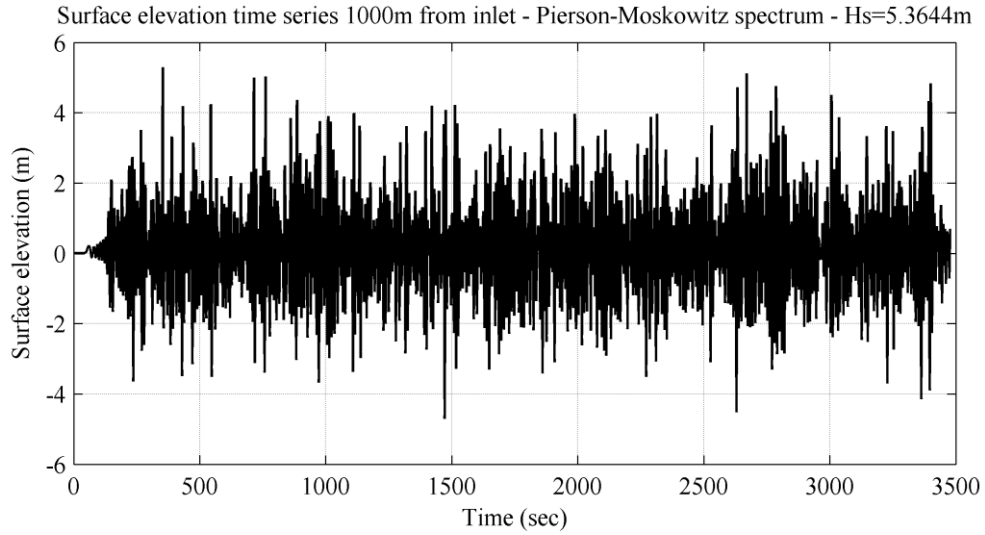

Figure 2. Surface elevation time series 1000m downstream from the inlet. Irregular wave condition generated from the Pierson-Moskowitz spectrum.

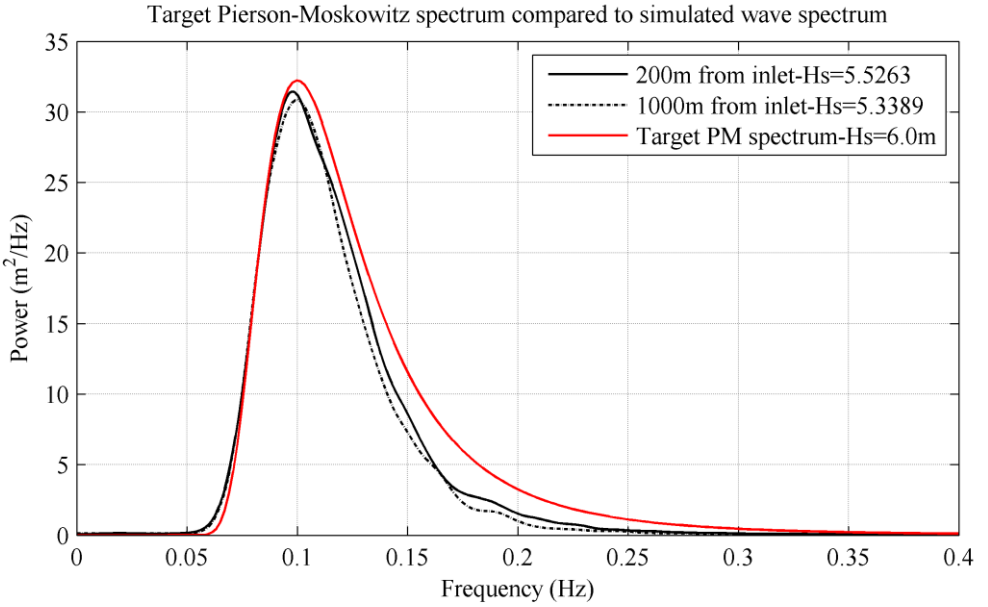

Figure 3. Target Pierson-Moskowitz wave spectrum for generation of irregular waves. Wave spectrum from simulated surface elevations at 200m and 1000m downstream the inlet.

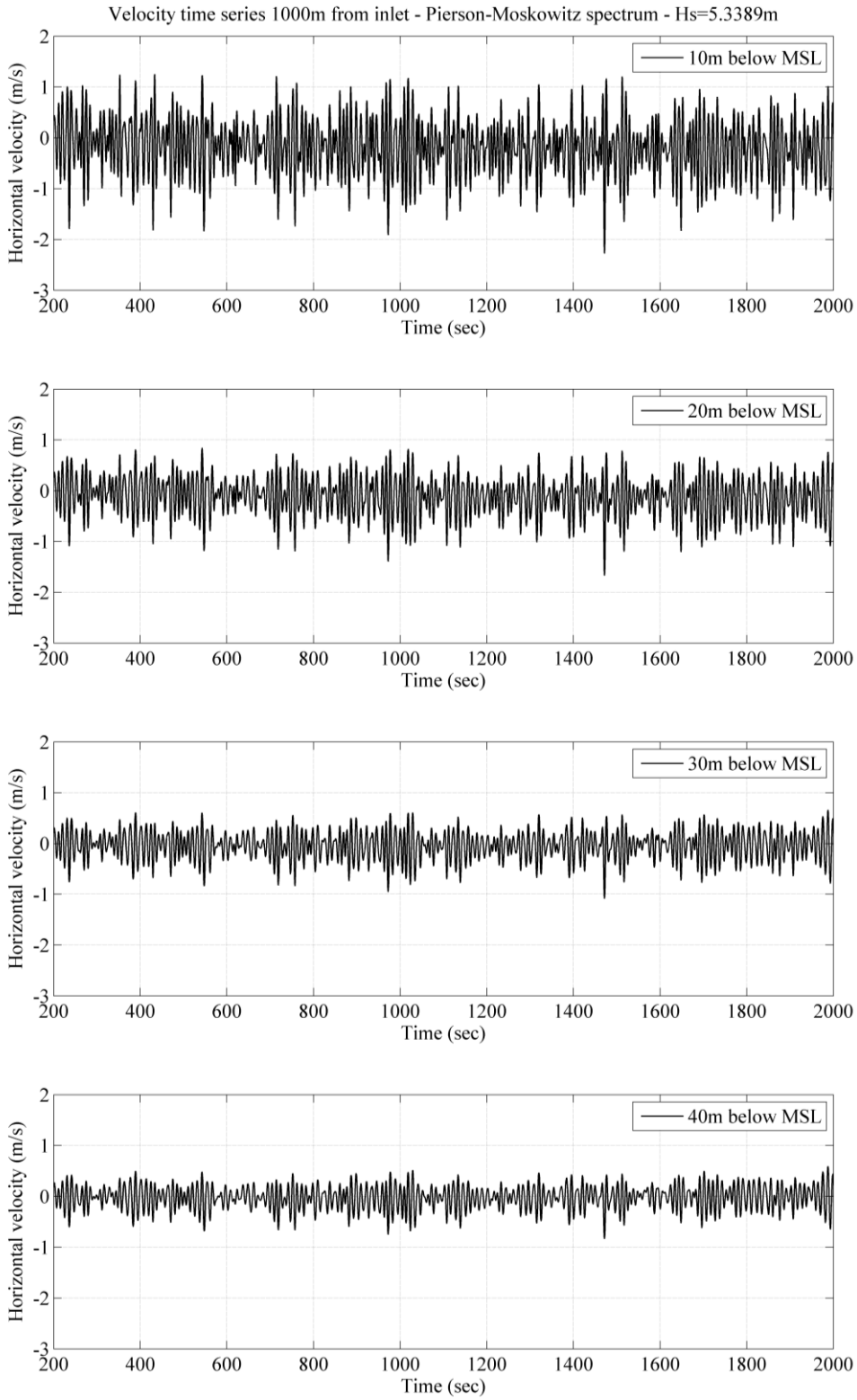

Figure 4. Horizontal velocity time series at 1000m downstream the inlet extracted from the model at 10m, 20m, 30m, and 40m below mean sea level.

Figure 4 presents the extracted horizontal velocity time series at four different levels below the mean sea level. As expected the magnitude is decreasing with increasing distance from the surface. The same variation of the velocities can be identified down through the individual time series. One extreme event can be identified between time 1400s and 1500s with a horizontal velocity which exceeds -2.5m/s. In order to examine this event in details with respect to the variation over the water depth a close-up of the time series is presented in Figure 5.

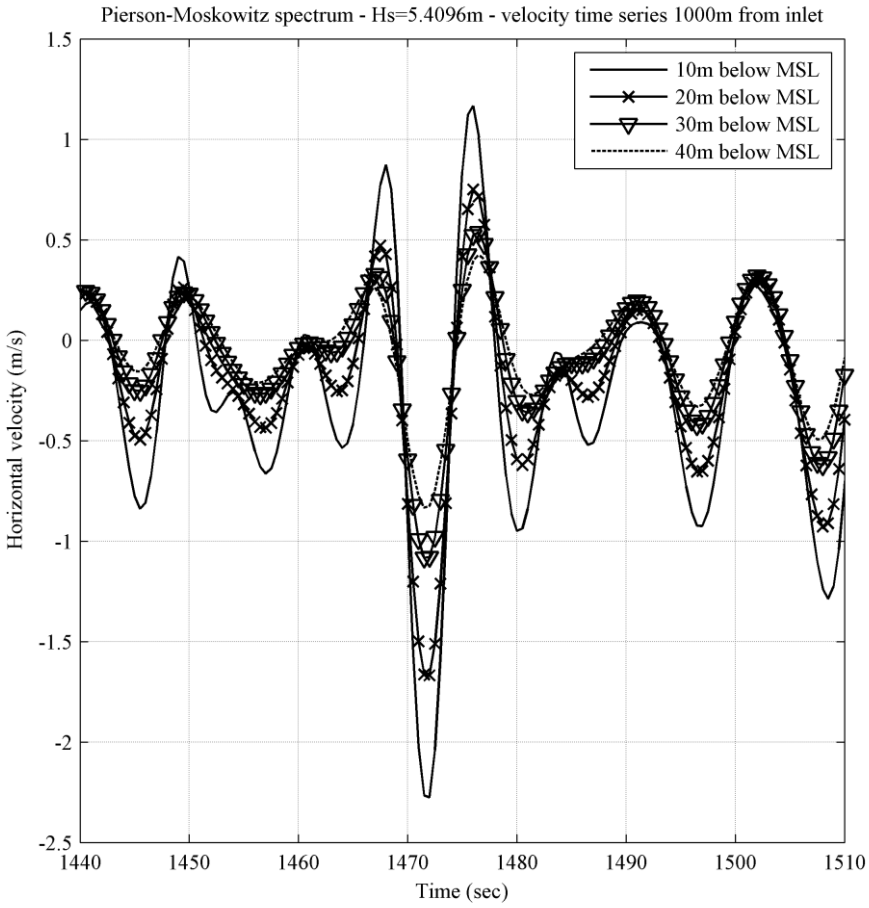

Figure 5. Close-up at horizontal velocity time series during event of large velocities.

4. FORCES ON VERTICAL CYLINDERS

The previous section showed examples of generation of wave kinematics for regular and irregular waves which may be used for assessment of loads on offshore structures in combination with the Morison-equation. An alternative approach is to apply the numerical model to simulate the loads directly on the structure i.e. the structure is included and resolved in the numerical grid. This methodology has been described and compared to conventional design methods for mono-piles in terms of Morison-equation in Christensen et al. (2007) where the NS3 code was used. The NS3 code has further been applied for loads on gravity based wind turbine foundation as described in Bredmose et al. (2006). Other structural applications have been reported in Mayer and Nielsen (2005) in terms of loads on rectangular beams and in Nielsen and Mayer (2004) where green water incidents on a ship deck were investigated. Based on the solid background of the NS3 code a reference simulation has been prepared in terms of wave loads on a vertical cylinder exposed to very steep non-linear waves. These results are used for comparison with the OpenFOAM model. The OpenFOAM model has recently been applied in combination with waves2Foam for simulation of wave impact on offshore wind turbine foundations as presented in Bredmose and Jacobsen (2010) and for wave loads on inspection platforms shown in Bredmose and Jacobsen (2011). All results are in the following furthermore compared to loads predicted by the Morison-equation.

A test case has been setup with the following characteristics. Cylinder diameter, D=6m, wave height, H=15.14m, wave period, T=11.75s, water depth, h=30m. The waves are generated as stream function waves and will for this case results in a Keulegan-Carpenter number of KC=15 and a Reynolds number of $Re=4.7*10^7$.

A rectangular model domain has been setup with a total length of 800m. At the inlet and outlet boundary a relaxation zone with a length of 200m is used for generating and absorbing the waves respectively. In the vertical direction uniform grid spacing is applied with a resolution at 0.86m. In the horizontal direction grid refinement is applied near the cylinder with a minimum resolution at 0.5m. A total of approximately 800,000 computational cells are applied. Forces on the cylinder are computed by integrating the pressure over the entire cylinder surface.

Figure 6 presents the results of the NS3 simulation in terms of in-line forces on the cylinder. The force variation follows with good agreement the previous results reported for mono-piles in Christensen et al. (2007). Furthermore the loads are calculated based on the Morison-equation in combination with the theoretical wave kinematic found from stream function theory. The comparison is also shown in Figure 6 where good agreement is found. The load coefficients applied in the Morison-equation are $C_D=0.7$ and $C_M=1.7$.

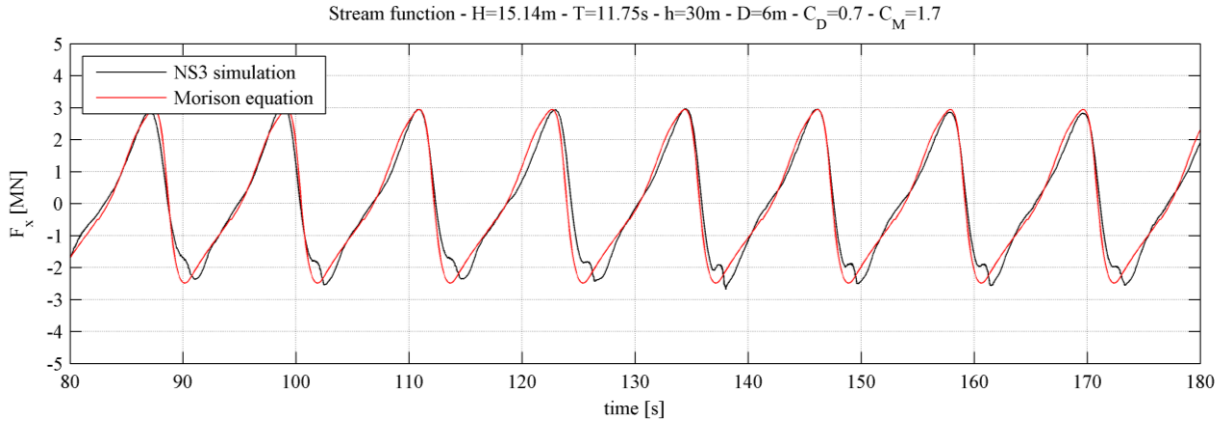

Figure 6. In-line forces from the NS3 simulation compared to Morison equation with stream function theory. H=15.14m, T=11.75s.

Following the reference simulation with the NS3 code a corresponding simulation is performed with the OpenFOAM code. The computational domain is identical to that applied for the NS3 simulations. The waves2Foam frame work is applied to generate a stream function wave with the same characteristics. The results are presented in Figure 7 as both the in-line forces on the cylinder as well as the surface elevation upstream the cylinder. Comparing to the NS3 results in Figure 6 it is seen how the forces show a very similar variation over time. Also the comparison to Morison-equation shows good agreement for the OpenFOAM model. It is noted that slightly higher forces are found in the OpenFOAM model compared to the NS3 model. The explanation for this is not found yet but it should be mentioned that the deviation is of a size where it cannot be conclusively determined whether the NS3 results or the OpenFOAM results are most correct. However the overall impression is that both models are capable of reproducing the forces within an acceptable accuracy.

In order to further verify the applicability of the OpenFOAM model it is suggested to perform similar simulations with decreasing wave steepness as well as include comparisons to experimental data in order to show some conclusive validation results. Furthermore the validation tests may be extended to include a caisson wind turbine foundation which has been evaluated through several projects with the NS3 code and as such a large amount of results exists for comparison.

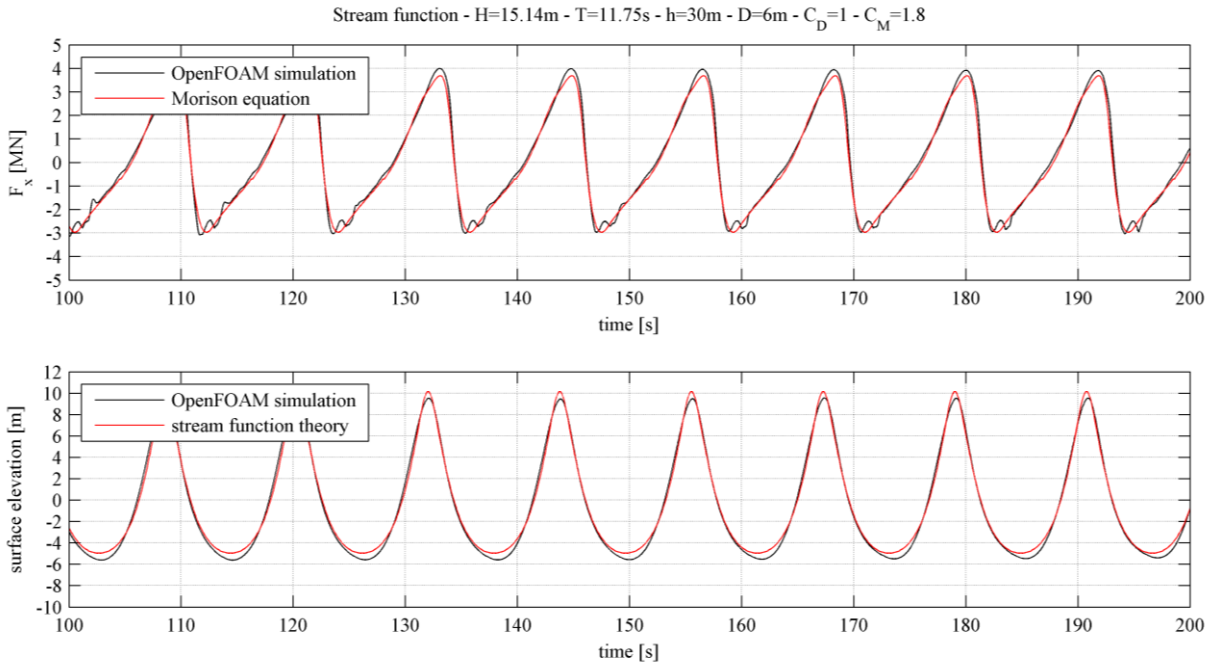

Figure 7. Results from the OpenFoam simulation compared to Morison equation with stream function theory. Top panel: in-line forces, bottom panel: surface elevation upstream cylinder. H=15.14m, T=11.75s.

5. RUN-UP ON VERTICAL CYLINDERS

From the simulations of forces on a vertical cylinder in very steep non-linear waves in the previous section it was seen that a large run-up occurs on the cylinder surface. This may be of interest for at least two reasons: i) the run-up is part of the pressure distribution on the cylinder surface and as such it contributes to the total in-line force, and ii) the run-up may course critical loads on secondary structures if not taken into account when designing and positioning these structures. The simulation of run-up on the vertical surface of a cylinder has previously been investigated by means of the NS3 code as described in Christensen and Hansen (2005) and in Nielsen et al. (2008).

In this section it is investigated how well the OpenFOAM model captures the run-up around a circular cylinder. Experimental data from Kriebel (1992) are used for comparison. These data were also used for the validation of the NS3 code in Christensen and Hansen (2005).

Figure 8 presents a definition sketch of the run-up around the cylinder. The incident wave is magnified as it interacts with the cylinder. Here the run-up, R, is defined as the distance from the mean sea level (MSL) to the position of the free surface on the cylinder at any given time and angular position around the cylinder. The run-up envelope is defined as shown in Figure 8 as the maximum free surface position which

has occurred during one wave period around the cylinder. The run-up envelope was experimentally recorded in Kriebel (1992) and will be compared to the numerical results from the OpenFOAM model.

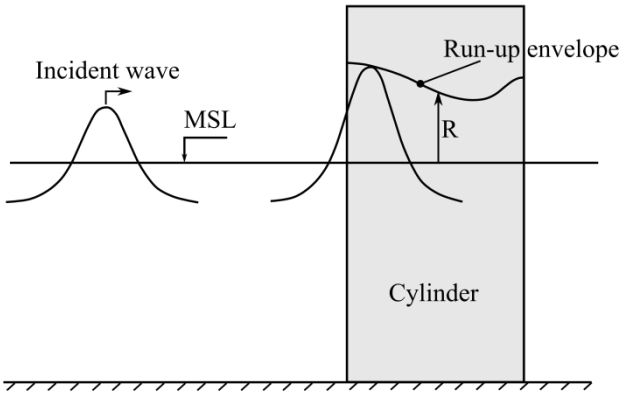

Figure 8.Definition sketch of run-up on a circular cylinder. After Kriebel (1992).

A rectangular model domain has been setup with dimensions corresponding to the experiments reported in Kriebel (1992). A sketch of the layout is shown in Figure 9. The cylinder had a diameter at D=0.32m and the water depth was h=0.45m for all experiments. Two cases have been simulated with regular Stokes 2nd order waves given as kH=0.215 (H=0.13m and T=1.95s) and kH=0.402 (H=0.17m and T=1.5s). At the inlet and outlet boundary a relaxation zone with a length of approximately 1 wave length is used for generating and absorbing the waves respectively.

In the vertical direction uniform grid spacing is applied with a resolution at 0.02m. In the horizontal direction grid refinement is applied near the cylinder with a minimum resolution at 0.01m. A total of approximately 700,000 computational cells are applied.

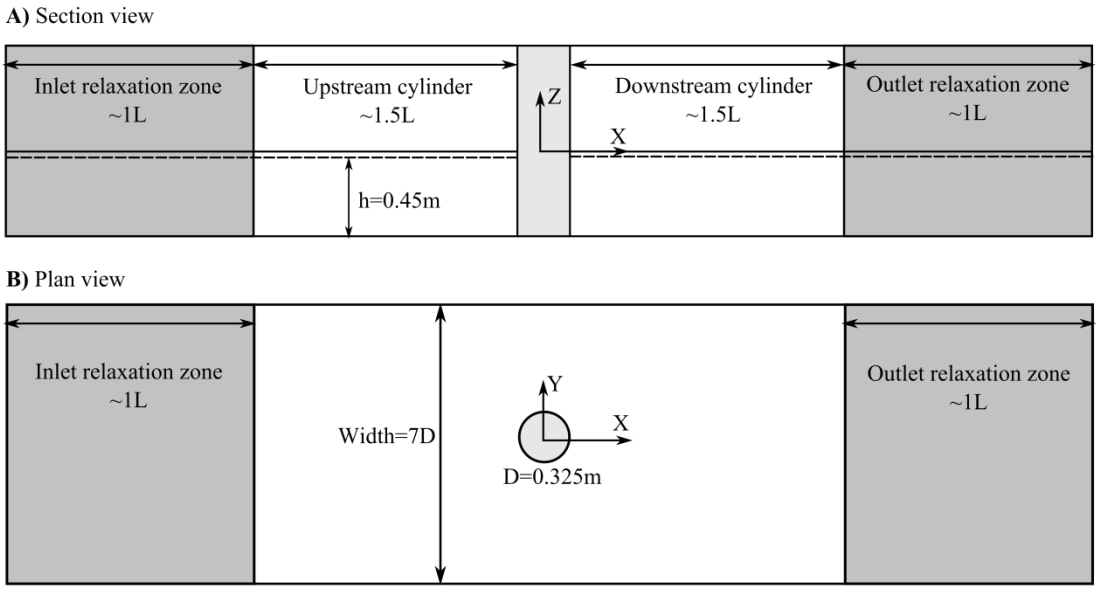

Figure 9. Sketch of the numerical model domain.

Figure 10 presents the results of the two cases with kH=0.215 and kH=0.402 respectively. The run-up, R, is normalized with H/2 in order to follow the notation in Kriebel (1992). The results are shown as time stamps of the surface elevation around the cylinder during one wave period. Experiments are shown as the envelope of the surface elevation i.e. the maximum position of the water surface at any angular position around the cylinder.

The simulated run-up is seen to be in good agreement with the experimental data. The maximum run-up is captured both on the leading edge (0deg) and trailing edge (180deg). For kH=0.402 some deviation is seen from 90deg-150deg where the maximum run-up is underestimated. However, the overall impression is that the model is capable of reproducing the measured run-up. Figure 11 and Figure 12 presents an iso-surface contour plot of the free surface around the cylinder at maximum run-up on the leading and trailing edge respectively.

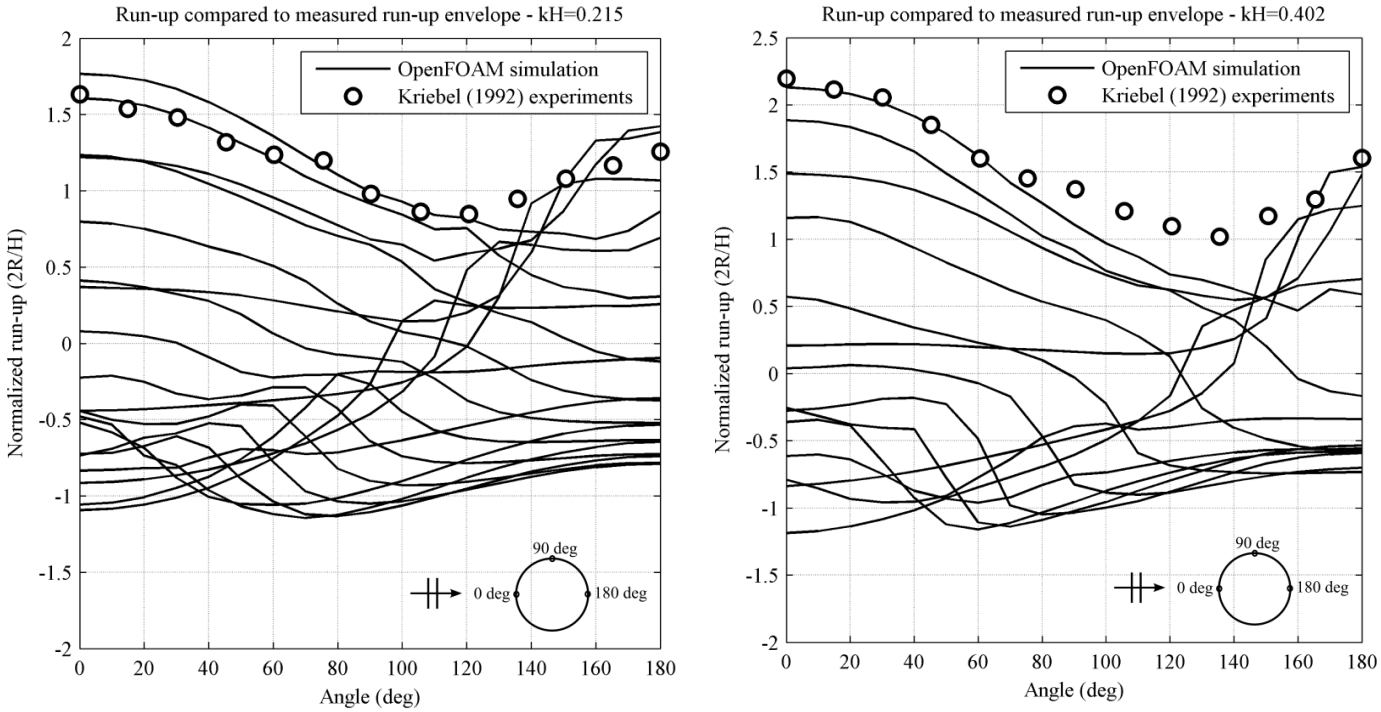

Figure 10. Results of run-up simulations compared to experimental data. Solid lines represent results of the numerical simulation as time stamps of the surface elevation around the cylinder during one wave period. Experimental data are shown as circles representing the envelope of the maximum surface elevation.

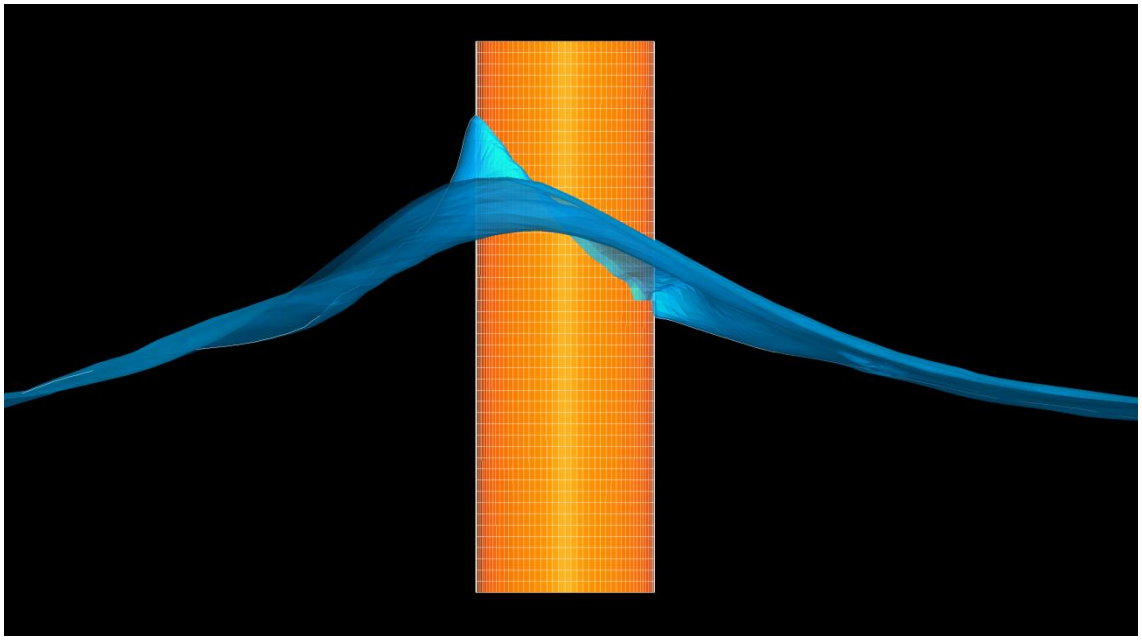

Figure 11. Maximum run-up at the leading edge for kH=0.402.

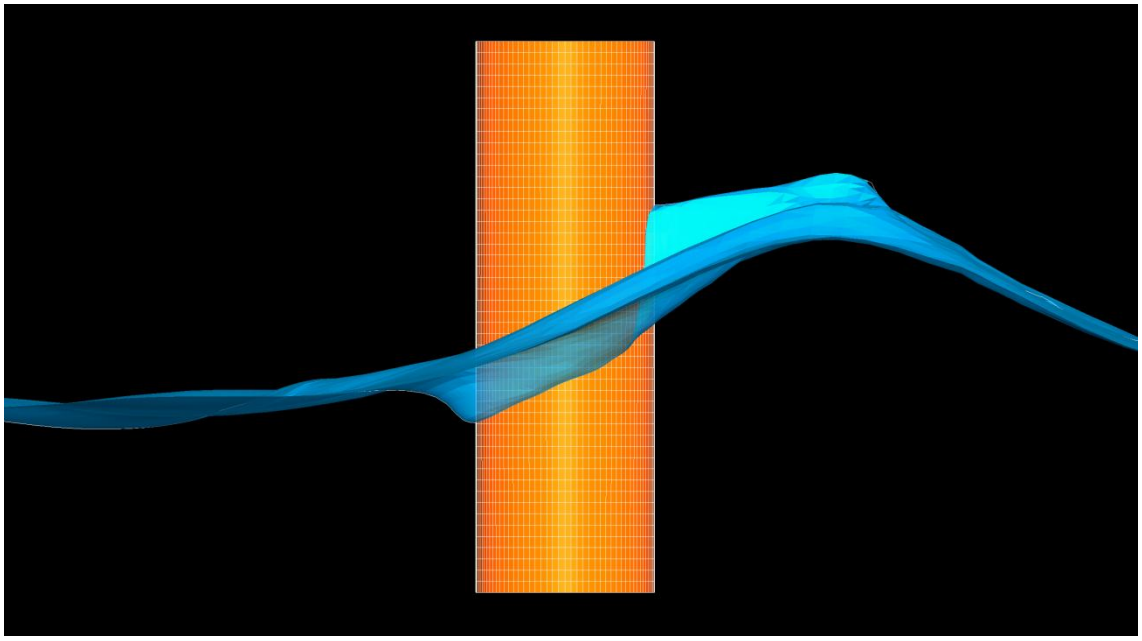

Figure 12. Maximum run-up at the trailing edge for kH=0.402.

6. REFERENCES

Bredmose, H., Skourup, J., Hansen, E. A., Christensen, E. D., Pedersen, L. M., & Mitzlaff, A. (2006). Numerical reproduction of extreme wave loads on a gravity wind turbine foundation. *International Conference on Offshore Mechanics and Arctic Engineering, OMAE* (pp. 1-9).

Bredmose, H. and Jacobsen, N. G. (2010). Breaking Wave Impacts on Offshore Wind Turbine Foundations: Focused Wave Groups and CFD. *Proceedings of the 29th ASME International Conference on Ocean, Offshore and Arctic Engineering*, Shanghai, China, **3**, 397-404

Bredmose, H. and Jacobsen, N. G. (2011). Vertical wave impacts on offshore wind turbine inspection platforms. *Proceedings of the 30th ASME International Conference on Ocean, Offshore and Arctic Engineering*, Rotterdam, The Netherlands (on CD)

Christensen, E. D., & Hansen, E. A. (2005). Extreme wave run-up on offshore wind-turbine foundations. *International Conference on Computational Methods in Marine Engineering* (pp. 1-10).

Christensen, E. D., Tarp-johansen, N. J., Yde, L., Gravesen, H., & Damsgaard, M. L. (2007). Wave loads on offshore wind turbine foundations in shallow water Engineering models vs . refined flow modeling. *EOW2007*.

Gronbech, J., Sterndorf, M. J., Gregorian, H., Jacobsen , V. (2001). Hydrodynamic Modelling of Wave-In-Deck Forces on Platform Decks. Offshore Technology Conference (OTC) 2001.

Hirt, C., & Nichols, B. (1981). Volume of fluid (VOF) method for the dynamics of free boundaries. *Journal of Computational Physics*, *39*(1), 201-225. doi:10.1016/0021-9991(81)90145-5

Kriebel, D. L. (1992). Nonlinear wave interaction with a vertical circular cylinder. Part II: wave run-up. *Ocean Engineering*, *19*(1), 75-99.

Jacobsen, N. G. (2011). A Full Hydro- and Morphodynamic Description of Breaker Bar Development. *Ph.D. Thesis*. DCAMM Special Report no. S136, Technical University of Denmark, Deparment of Mechanical Engineering.

Jacobsen, N. G., Fuhrman, D. R., & Fredsøe, J. (2011). A wave generation toolbox for the open-source CFD library : OpenFoam. *International Journal for Numerical Methods in Fluids*. doi:10.1002/fld

Mayer, S., Garapon, A., & Sørensen, L. S. (1998). A fractional step method for unsteady free-surface flow with applications to non-linear wave dynamics. *International journal for numerical methods in fluids*, *315*(28), 293-315.

Mayer, S., & Nielsen, K. B. (2005). Numerical prediction of wave impact loads on multiple rectangular beams. *Coastal Engineering Journal*, *47*(1), 41-65.

Nielsen, A. W., Mortensen, S. B., Jacobsen, V., & Christensen, E. D. (2008). Numerical Modelling of Wave Run-Up on a Wind Turbine Foundation. ASME. doi:10.1115/OMAE2008-57224

Nielsen, K. B., & Mayer, S. (2004). Numerical prediction of green water incidents. *Ocean Engineering*, *31*(3-4), 363-399. doi:10.1016/j.oceaneng.2003.06.001

Sterndorff , M. J. (2002). Large-Scale Model Tests with Wave Loading on Offshore Pltaform Deck Elements. Proceedings of OMAE´02 21st International Conference on Offshore Mechanics and Artic Engineering, OMAE 2002.

APPENDIX2: fvSolution and fvSchemes

fvSolution:

```
/*---------------------------------*- C++ -*----------------------------------*\
| =========                 |                                                 |
| \\      /  F ield         | OpenFOAM: The Open Source CFD Toolbox           |
|  \\    /   O peration     | Version:  1.5                                   |
|   \\  /    A nd           | Web:      http://www.OpenFOAM.org               |
|    \\/     M anipulation  |                                                 |
\*---------------------------------------------------------------------------*/
FoamFile
{
    version     2.0;
    format      ascii;
    class       dictionary;
    object      fvSolution;
}
// * * * * * * * * * * * * * * * * * * * * * * * * * * * * * * * * * * * * //

solvers
{
/*    pcorr PCG
    {
        preconditioner   DIC;
        tolerance       1e-10;
        relTol          0;
    };
    pd PCG
    {
        preconditioner   DIC;
        tolerance       1e-7;
        relTol          0.001;
    };
    pdFinal PCG
    {
        preconditioner   DIC;
        tolerance       1e-7;
        relTol          0;
    };*/

    pcorr
    {
        solver          GAMG;
        tolerance       1e-7;
        relTol          0.0;

        smoother        DIC;//GaussSeidel;
        nPreSweeps      0;
        nPostSweeps     2;
        nFinestSweeps   2;

        cacheAgglomeration true;
        nCellsInCoarsestLevel 10;
        agglomerator    faceAreaPair;
```

```
    mergeLevels     1;
};

pd
{
    solver          GAMG;
    tolerance       1e-7;
    relTol          0.0;

    smoother        DIC;//GaussSeidel;
    nPreSweeps      0;
    nPostSweeps     2;
    nFinestSweeps   2;

    cacheAgglomeration true;
    nCellsInCoarsestLevel 10;
    agglomerator    faceAreaPair;
    mergeLevels     1;
};

pdFinal
{
    solver          GAMG;
    tolerance       1e-8;
    relTol          0.0;

    smoother        DIC;//GaussSeidel;
    nPreSweeps      0;
    nPostSweeps     2;
    nFinestSweeps   2;

    cacheAgglomeration true;
    nCellsInCoarsestLevel 10;
    agglomerator    faceAreaPair;
    mergeLevels     1;
};

U
{
    solver          PBiCG;
    preconditioner  DILU;
    tolerance       1e-09;
    relTol          0;
};

UFinal
{
    solver          PBiCG;
    preconditioner  DILU;
    tolerance       1e-09;
    relTol          0;
};

alpha1
{
    solver          BiCGStab;
    preconditioner  Cholesky;
```

```
    minIter         0;
    maxIter         500;
    tolerance       1e-8;
    relTol          0.0;
  };


}

PISO
{
  pdRefCell 0;
  pdRefValue 0;
  momentumPredictor yes;
  nOuterCorrectors 1;
  nCorrectors    3;
  nNonOrthogonalCorrectors 1;
  nAlphaCorr     1;
  nAlphaSubCycles 1;
  cAlpha         1;
}

// ************************************************************************* //
```

fvScheme

```
/*--------------------------------*- C++ -*----------------------------------*\
| =========                 |                                                 |
| \\      /  F ield         | OpenFOAM: The Open Source CFD Toolbox           |
| \\    /   O peration     | Version:  1.5                                   |
|  \\  /    A nd           | Web:      http://www.OpenFOAM.org               |
|   \\/     M anipulation  |                                                 |
\*---------------------------------------------------------------------------*/
FoamFile
{
  version    2.0;
  format     ascii;
  class      dictionary;
  object     fvSchemes;
}
// * * * * * * * * * * * * * * * * * * * * * * * * * * * * * * * * * * * * //

ddtSchemes
{
  default Euler;
}

gradSchemes
{
  default       Gauss linear;
  grad(U)       Gauss linear;
  grad(alpha1)    Gauss linear;
}

divSchemes
{
  div(rho*phi,U)  Gauss linearUpwindV cellMDLimited Gauss linear 1.0;
```

```
    div(phi,alpha)  Gauss Gamma 0.1;
    div(phirb,alpha) Gauss interfaceCompression;
}

laplacianSchemes
{
    default       Gauss linear corrected;
}

interpolationSchemes
{
    default       linear;
}

snGradSchemes
{
    default       corrected;
}

fluxRequired
{
    default       no;
    pd;
    pcorr;
    alpha1;
    p;
}

// ************************************************************************* //
```

APPENDIX3: Brief Investigation of Numerical Schemes for Velocity Divergence Term

Tests to see if by altering the numerical scheme for the velocity convection term in the Navier-Stokes equation (div(rho*phi,U) in OpenFOAM notation) had an effect. For the work presented in the previous section the div(rho*phi,U) was solved using "**Gauss linearUpwindV cellMDLimited Gauss linear 1.0**" a 2^{nd} order upwind scheme with cell limiters. Model tests all used Mesh 1 (Table 1) and solved div(rho*phi,U) using other OpenFoam scheme options. '**Gauss linearUpwind cellLimited Gauss linear 1.0**' was tested which is a variation in limiters to '**Gauss linearUpwindV cellMDLimited Gauss linear 1.0**'. **LimitedLinearV 1.0**, a second order central differencing scheme, which could be considered to be less diffusive than the second order Upwind scheme and **SFCDV** a blended upwind / central scheme of second order and were also both tested.

The model run using the **SFCDV** scheme was not successful due to a numerical instability in the velocity calculation causing the simulation to stop well before 200seconds simulated time.

The model run using **LimitedLinearV 1.0** showed spurious high velocities in the air phase (some as high as 50m/s) , which appeared to have a distortive affect to the free surface. Figure 6 plots a section of the numerical flume (1100-1300m downstream of the inlet) at time 200seconds. From the figure it is apparent that the velocities in the air phase have an undesirable effect on the shape of the free surface as well as the neighboring velocities in the water phase.

Figure 7 shows the negligible difference between using the '**Gauss linearUpwind cellLimited Gauss linear 1'** and '**Gauss linearUpwindV cellMDLimited Gauss linear 1.0**' with regard to the high velocities near the top close to the free surface.

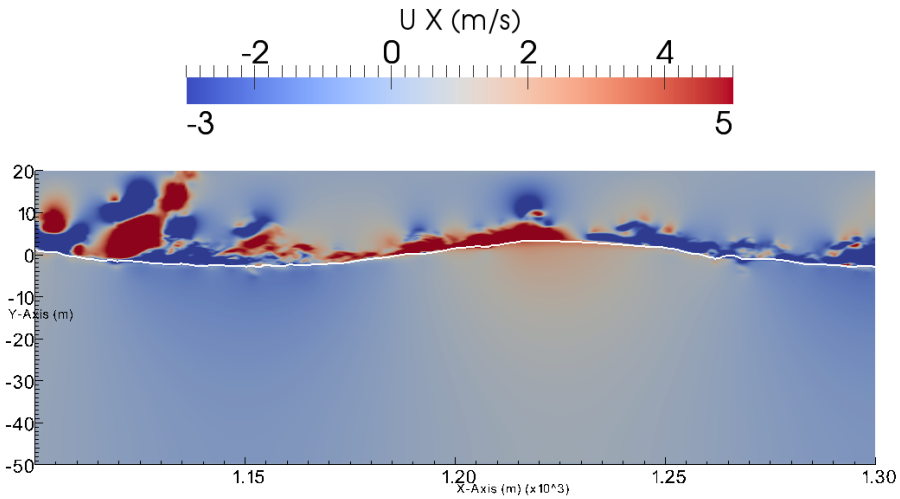

Figure 6: Contour plot of horizontal velocity for a portion of the numerical flume (1100-1300m) at time 200s of the simulation for a propagating streamfunction wave (H=6m, h=50m, T=10s). The white line indicates the free surface. Testing the LimitedLinearV 1.0 scheme for the div(rho*phi,U) term. (Mesh1)

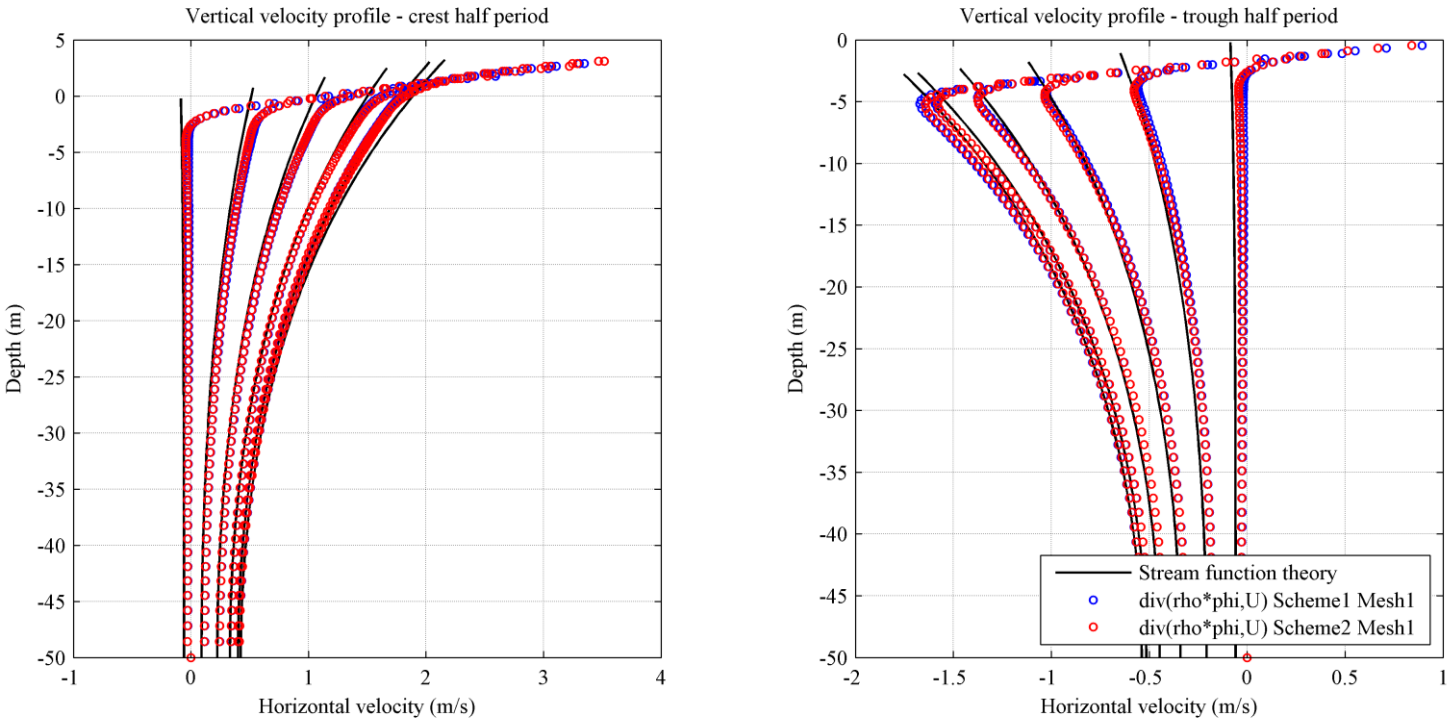

Figure 7: Figure 3: Horizontal velocities with respect to height from a vertical probe 1200m downstream of the flume inlet. Plots show comparisons between Scheme1 (Gauss linearUpwindV cellMDLimited Gauss linear 1.0) and scheme2 (Gauss linearUpwind cellLimited Gauss linear 1.0) for the dive(rho*phi,U) term in waveFoam implemented in OpenFOAM1.6-ext against streamfunction theory. Plots are spaced with a 0.5s interval. A) Crest half period. B) Trough half period.

It should be noted that the tests in this section are only altering one of the divergence schemes at a time and observing the results. The results could differ with respect to mesh quality as well as the selection of other numerical schemes for other terms other than div(rho*phi,U).

BILAG B– Bølger på Dæk

Verifikation af Bølger på Dæk model

Verification of Wave-in-Deck model

Introduction

This note describes the simulations carried out with DHI's inhouse Wave-in-Deck (WiD) model in order to benchmark it against the IEA Annex 30 project partner's various aero-elastic codes. For this reason, the jacket structure defined for offshore code comparison during phase I of the OC4 project under IEA Wind Annex XXX. Full description of the jacket is found in /1/.

Model Setup

The model is setup up in the program Wave-in-Deck. The program is designed to calculate the wave forces on a platform cellar deck caused by an impact of an extreme wave. The program do for this reason not include all the features to calculate all the probes requested. The main limitations of the program are that the program is made to calculated the forces on the structure and not response of the structure (shear forces, deflection etc.) and that the program are unable to include other forces than the hydrodynamic force. This includes the weight of the structure, buoyancy and external forces (for example the weight of the wind turbine).

The jacket foundation was set up using tubular for the entire structure as the transition piece was omitted. The transition piece can be omitted as this part of the structure is not hit by the waves and as the program do not include structural responds there is no effect including the transition piece. The jacket is shown in Figure 1.

The legs of the platform are modeled as "vertical tubular" and all the bracing are modeled as "horizontal tubular".

A regular airy wave of 6 m high and 10 s long was applied as specified for load case 2.3a (/2/). The water was kept constant at 50 m.

Results

The results are extracted from the model at pre-defined points (probes). The definition of the individual probes are given in /2/.

The following probes were found relevant to compare: 5, 53, 54, 55, 56 and 57. The results for each of the probes are discussed and compared with the results for other codes. In the plots the results from other codes are shown in gray, while the results obtained from Wave-in-Deck are red.

Probe 5 – Wave Elevation

The wave elevation does match for all the tested codes, including Wave-in-Deck.

Probe 53 – Fore-Aft Base Shear

There is a good correlation between Wave-in-Deck and the other codes when it comes to the phase of the oscillatory force. In the case of the amplitude of the force the result is in the lower range, but still within the range of the other codes.

Probe 54 – Side-To-Side Base Shear

The force is unexpectedly large, but still small compared to forces in the other directions. It has not been possible to find a reasonable explanation for the difference to the expected results and the other codes. The code has been tested for a structure without marine growth. In that case the side-to-side base shear was almost 0 kN.

Probe 55 – Overturning Moment around global x-axis

This moment is small for all other codes. Wave-in-Deck gives an unexpectedly large magnitude of the moment. This is clearly associated with the corresponding force (Probe 54).

Probe 56 – Overturning Moment around global y-axis

As in the case of Probe 53, there is a good agreement between Wave-in-Deck and the other codes for the phase. The amplitude is within the results from the other code, but while most of the other codes seem to have slightly larger negative moments than positive it is opposite for Wave-in-Deck.

Probe 57 – Moment around global z-axis at mudline

All the codes come up with small moments, except Wave-in-Deck. When compared to the results of probe 54 and 55 it can indicate that there is in the structure causing some asymmetry. It has not been possible to identify such kind of error, but the structure was also test without marine growth where the results of probe 54, 55 and 57 was very close to zero.

Conclusions

The overall forces on the structure were within the results of the other codes in the wave direction. The forces perpendicular to the wave direction are too large. It has not been possible to find the reason, but it might be an error in the marine growth as it is not a problem when the model is tested without marine growth.

References

/1/ Fabian Vorpahl, Daniel Kaufer, *Description of a basic model of the "Upwind reference jacket" for code comparison in the OC4 project under IEA Wind Annex XXX*, Fraunhofer Institute for Wind Energy and Energy System Technology (IWES), September, 14, 2010

/2/ Fabian Vorpahl, Wojciech Popko, *Description of the Load Cases and Output Sensors to be simulated in the OC4 project under IEA Wind Annex XXX*, Fraunhofer Institute for Wind Energy and Energy System Technology (IWES), February 4, 2011

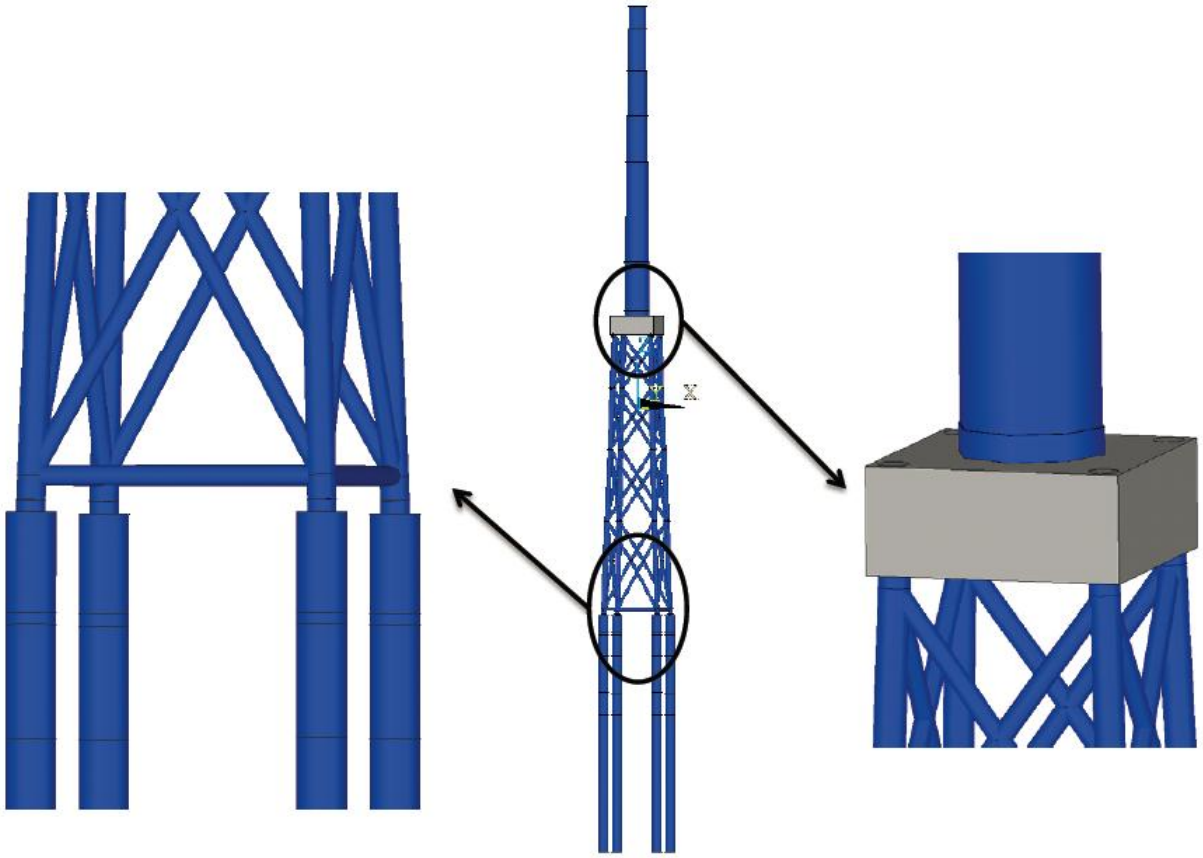

/4/ Figure 1 Jacket model (/1/)

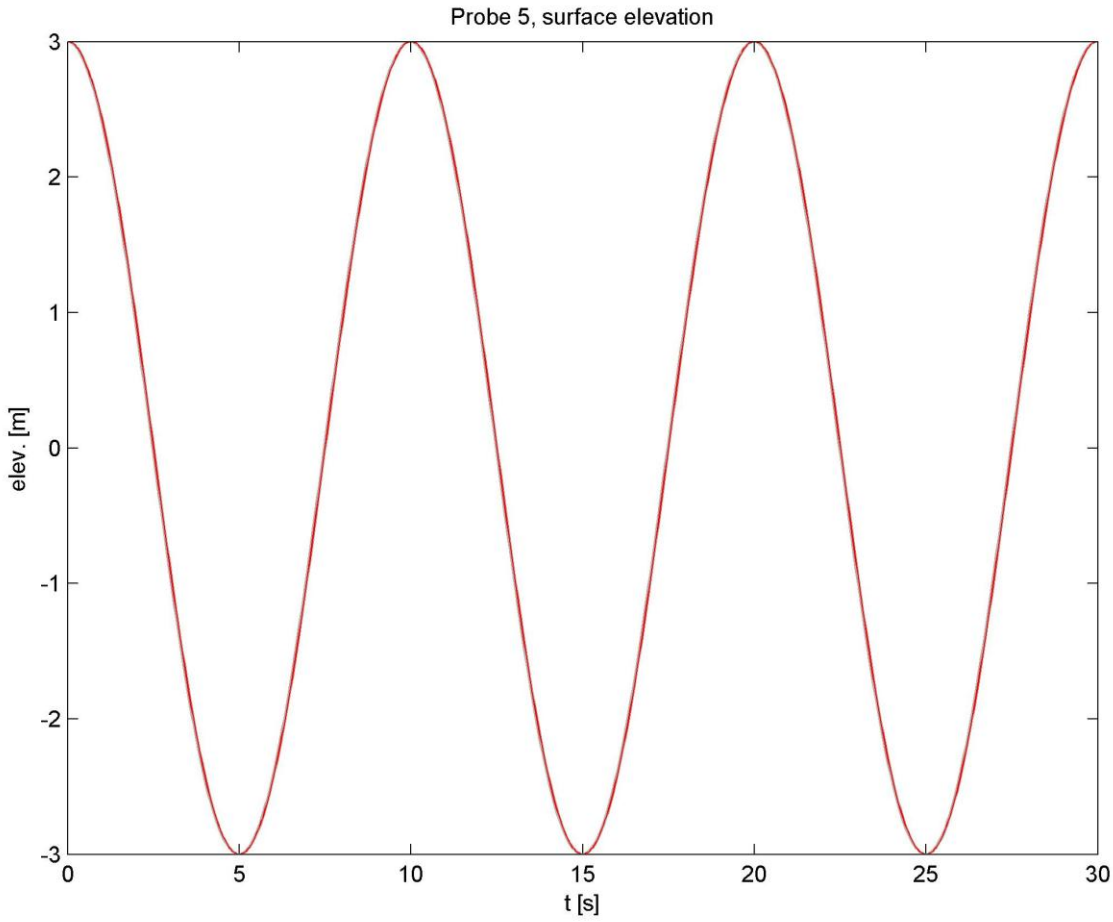

Figure 2 Probe 5 – Surface elevation

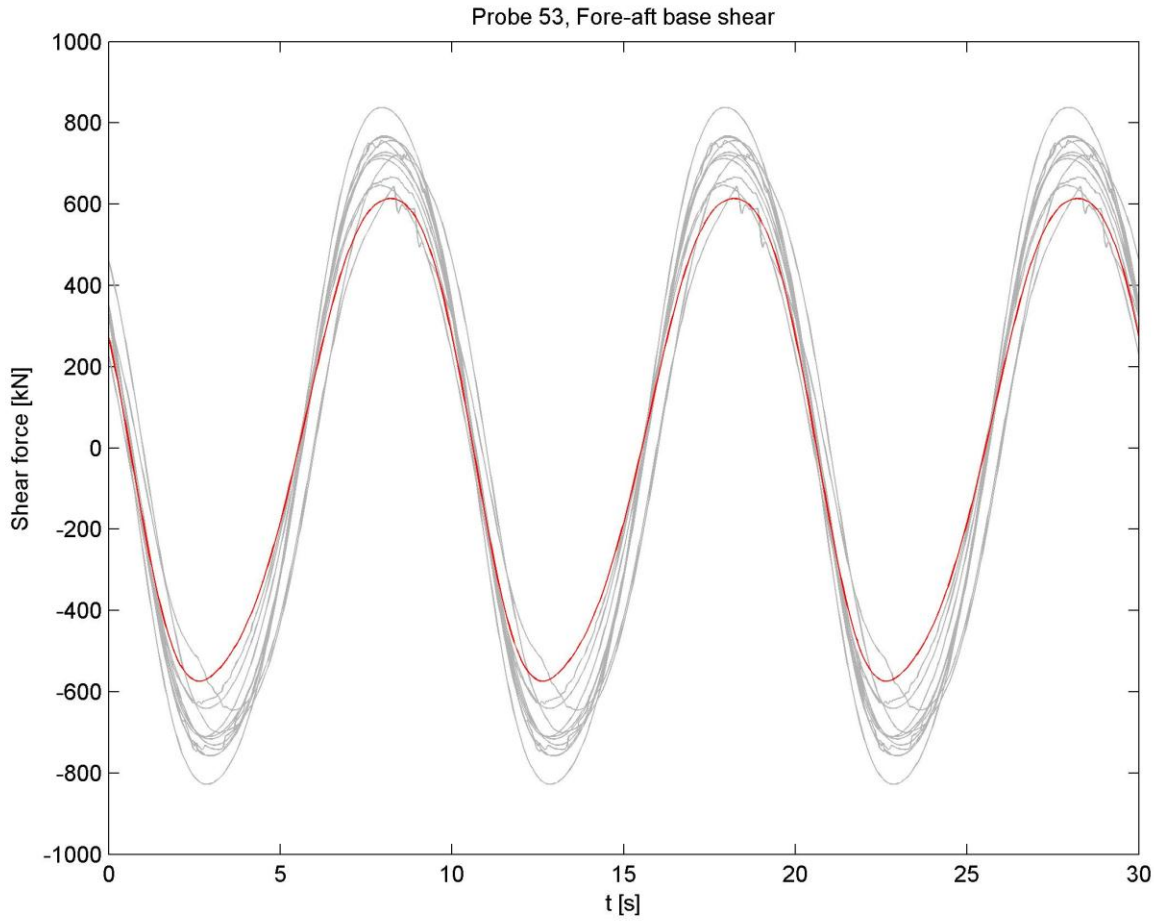

Figure 3 Probe 53 – Fore-aft base shear

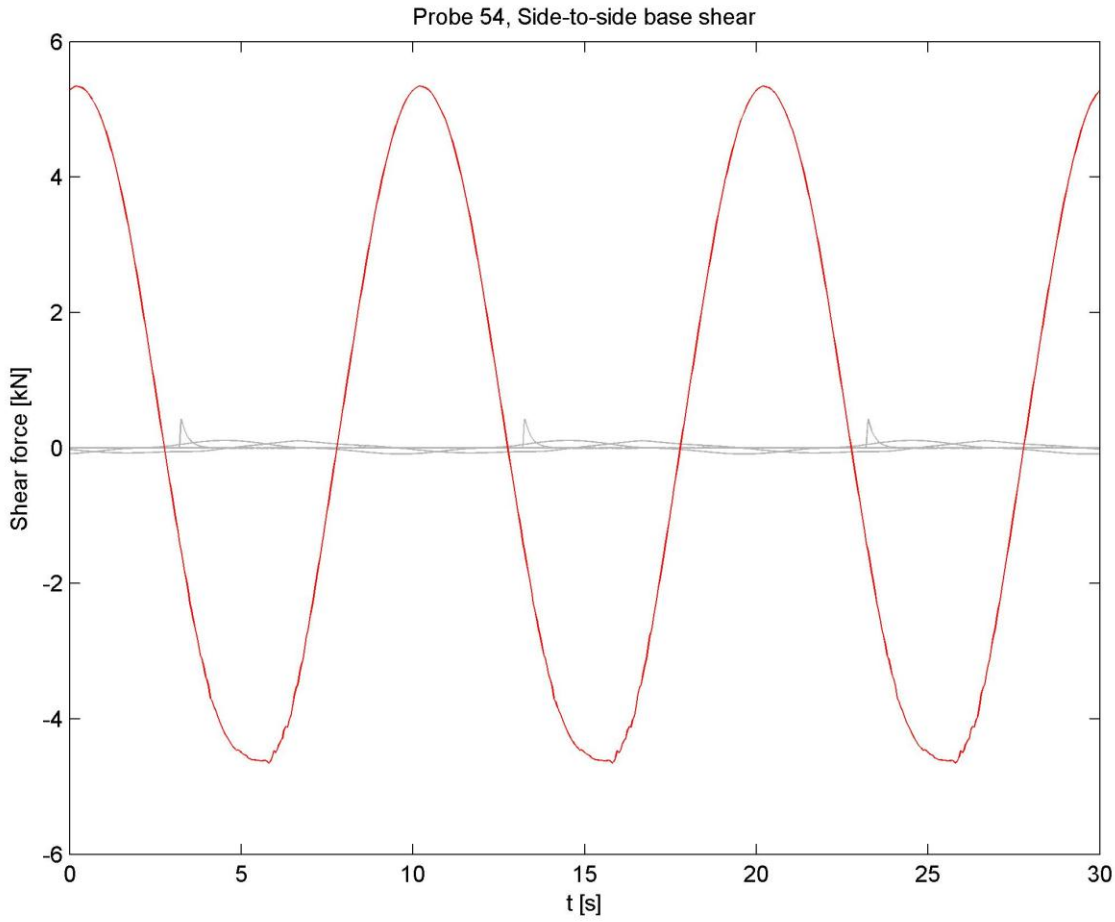

Figure 4 Probe 54 – Side-to-side base shear

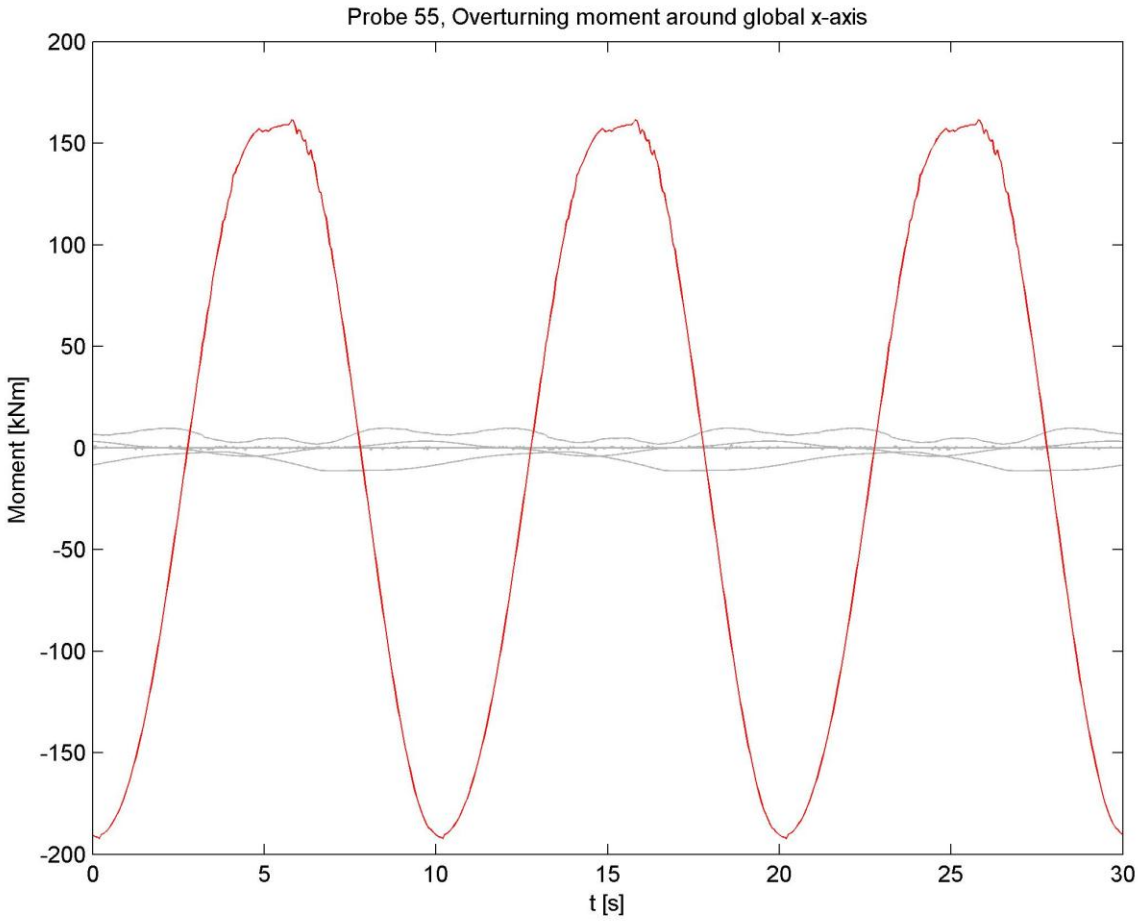

Figure 5 Probe 55 – Overturning moment around global x-axis

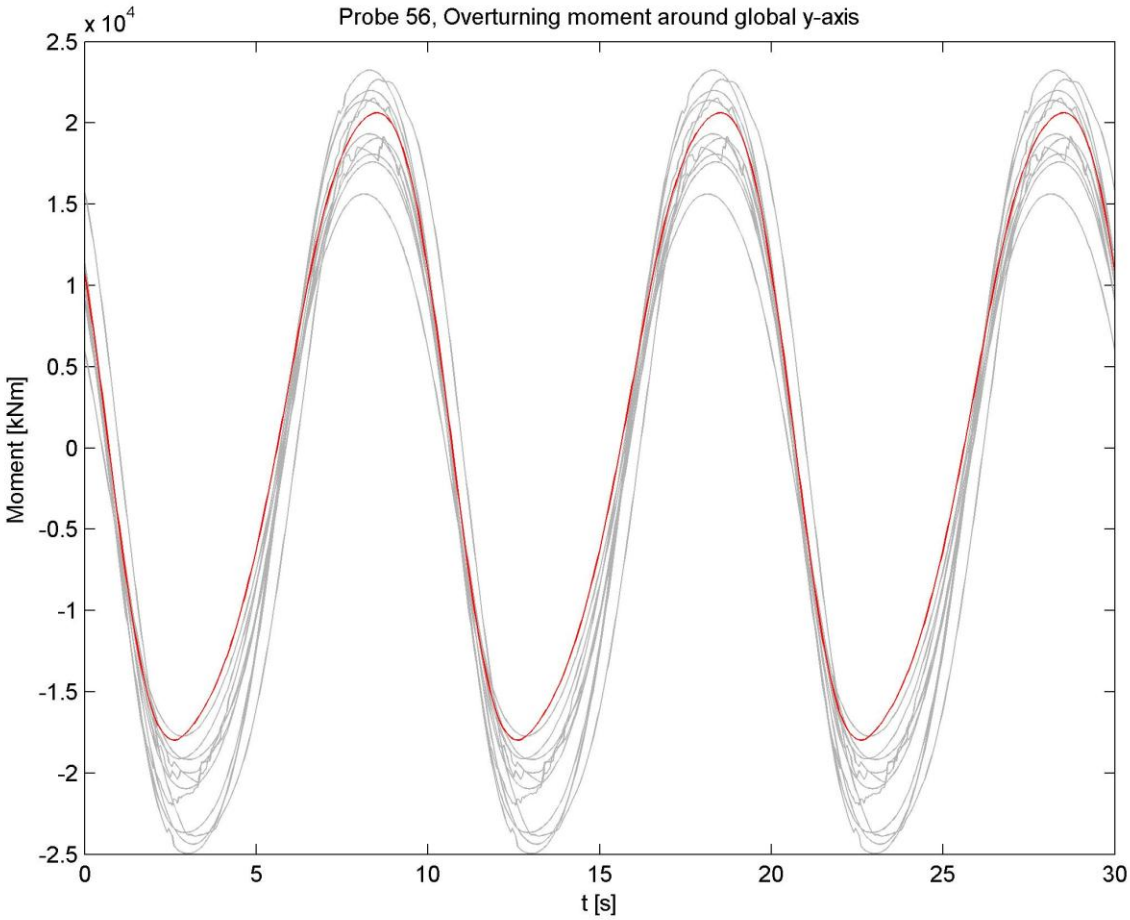

Figure 6 Probe 56 – Overturning moment around global y-axis

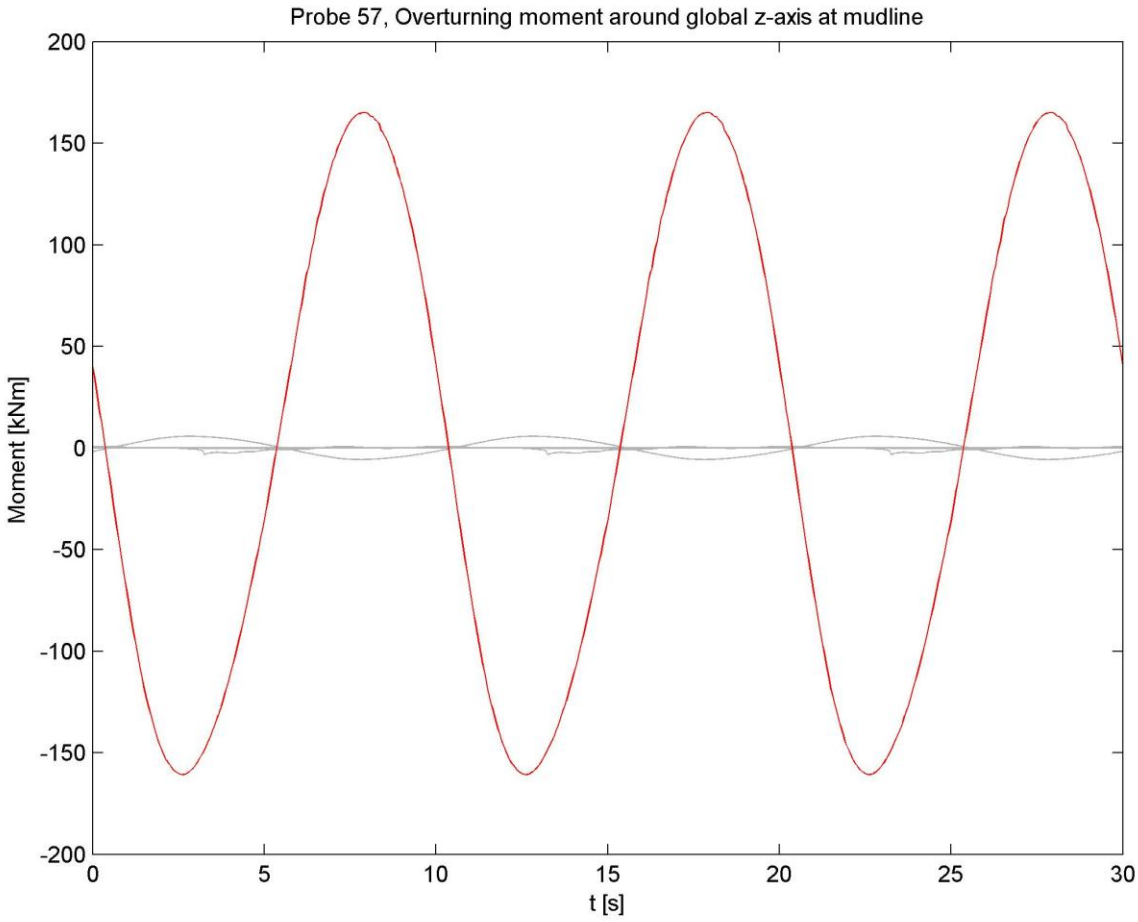

Figure 7 Probe 57 – Overturning moment around global z-axis at mudline